NIST

United States Department of Commerce
Technology Administration
National Institute of Standards and Technology

NIST Technical Note 1378

Optical Fiber, Fiber Coating, and Connector Ferrule Geometry: Results of Interlaboratory Comparisons

Timothy J. Drapela
Douglas L. Franzen
Matt Young

Optical Fiber, Fiber Coating, and Connector Ferrule Geometry: Results of Interlaboratory Measurement Comparisons

Timothy J. Drapela
Douglas L. Franzen
Matt Young

Optoelectronics Division
Electronics and Electrical Engineering Laboratory
National Institute of Standards and Technology
325 Broadway
Boulder, Colorado 80303-3328

CONTENTS

Optical Fiber, Fiber Coating, and Connector Ferrule Geometry: Results of Interlaboratory Measurement Comparisons

Timothy J. Drapela, Douglas L. Franzen, and Matt Young

National Institute of Standards and Technology[*]
Boulder, CO 80303-3328

Interlaboratory measurement comparisons, dealing with geometrical parameters of optical fibers, fiber coatings, and fiber connector ferrules (including steel pin gages used to determine ferrule inside diameter), have been coordinated by NIST. The international fiber (glass) geometry comparison showed better agreement among participants, for all measured parameters, than in previous comparisons. Many participants' test sets were calibrated for fiber cladding diameter measurements by means of calibration artifacts from NIST or other national standards laboratories; there was significantly better agreement among those participants than among participants whose test sets were not calibrated. In the other comparisons, some parameters showed large systematic offsets between participants' data; accurate calibration, for those parameters, would lead to better interlaboratory agreement. NIST is developing ferrule, pin gage, and coating calibration artifacts.

Key words: calibration; fiber coatings; fiber connector ferrule; geometry; geometrical parameters; optical fiber; pin gage.

1. Introduction

Geometrical parameters of optical fibers and fiber connector ferrules have received increasing attention as the industry has moved toward more efficient coupling between spliced or connected fibers. For typical single-mode telecommunications fibers, a transverse offset of as little as 1 µm between cores of joined fibers can cause insertion loss on the order of 0.2 dB. The trend in the industry has been toward tighter tolerances on specifications of geometrical parameters. This requires closer agreement among those in the industry, which, in turn, requires improved accuracy of the measurement methods.

---

[*]Fiber and Integrated Optics Group, Optoelectronics Division, Electronics and Electrical Engineering Laboratory.

Since 1988, the National Institute of Standards and Technology (NIST) has been coordinating interlaboratory measurement comparisons for various geometrical parameters. Each comparison involved measurements among members of either the Telecommunications Industry Association (TIA) for the North American comparisons, or the International Telecommunications Union (ITU, formerly the Consultative Committee on International Telegraph and Telephony, CCITT) for the international comparison. Here, we report on five interlaboratory comparisons, completed in 1994 and 1995, dealing with: fiber (glass) geometry; fiber coating geometry; ferrule inside (bore) diameter; pin gage (used to size the inside diameter of ferrules) diameter; and ferrule geometry.

For most of the parameters measured in the comparisons, we report what we call average measurement spread. We obtain this number, for a given parameter, by calculating the sample standard deviation for measurements on each measurement specimen, then calculating the arithmetic average of these standard deviations. The average measurement spread is not a statistically valid estimate of the overall spread of the population of all measurements on all specimens (such as a pooled standard deviation, which could not be meaningfully calculated for about half of the parameters reported here, due to large variations in standard deviations between specimens). Nevertheless, the average measurement spread estimates the standard deviation for the *average* measurement specimen and, hence, gives an indication of the relative agreement among participants.

2. Fiber (Glass) Geometry

This interlaboratory comparison of measurements of the geometrical parameters of bare fibers (cladding diameter, cladding noncircularity, and core/cladding concentricity error) was the third in a series of fiber geometry comparisons. Of the three parameters, cladding diameter was of most urgent interest. The industry was moving toward tolerances of ±1 µm on the nominally 125 µm cladding diameter specification [1] (down from a typical ±2 µm, before these comparisons started). To comfortably meet these tighter tolerances, agreement and, hence, accuracy on the order of ±0.1 µm were needed. Before giving results of the third and final comparison, we will briefly summarize previous results.

In 1989, the CCITT completed and reported on an international interlaboratory comparison of fiber geometry measurements [2]. The average measurement spread per fiber for mean cladding diameter was 0.38 µm and was deemed to be unacceptably high. Each participant received a separate set of fiber specimens, so all of the measurements were not

made on the same fiber ends. Longitudinal nonuniformity (taper) could therefore have influenced the results. The high measurement spread pointed to the need for all measurements to be made on the *same* cleaved fiber ends and also to the desirability of some type of calibration artifact [3].

In North America, NIST coordinated a second interlaboratory comparison for the TIA and reported results in 1992 [4]. Participants serially measured the same cleaved fiber ends, which could be retracted into aluminum housings for protection between measurements and during shipping. These housings use a brass barrel that is moved to extend or retract the fiber and is marked to identify the angular orientation of the fiber. The housed fiber specimens became the basis for the NIST calibration artifact or Standard Reference Material (SRM), which became available to the industry in late 1992 as SRM 2520 [5]. A diagram of the housing is shown in figure 1.

The average measurement spread per fiber for mean cladding diameter measurements in the 1992 comparison improved to 0.15 μm. There were also reductions in the measurement spreads for cladding noncircularity and core/cladding concentricity error. Participants' cladding diameter measurements were also compared to measurements made by the NIST contact micrometer, which is the measurement method for characterization and certification of the SRMs. The contact micrometer is accurate within ±0.045 μm (3 standard deviations) for mean cladding diameter measurements on the housed specimens [6]. The cladding diameter measurement spread observed in the 1992 study was largely due to systematic differences among participants, and further improvement in this spread was anticipated with the use of calibration artifacts such as the NIST SRMs.

NIST administered the most recent ITU international comparison, with help from regional coordinators in Europe and Japan. Housed fiber specimens were again used. Because the housed fibers could become damaged with repeated shipping, and in order to complete this comparison in a short time, three sets of specimens were prepared for three different regions: North America (A), Europe (E), and Pacific (P). Each set contained seven housed fiber specimens, including both very nearly circular (less than 0.1 percent noncircularity) and noncircular (up to 1.5 percent) fibers. To allow for inter-regional comparison, all fiber specimens were measured with the NIST contact micrometer. A total of 25 participants reported results. Of those, 23 used the gray scale measurement method [7], and two used image shearing [8]. Of the participants using the gray scale method, three used home-made test sets, while the others used test sets from commercial vendors.

Table 1 shows the measurement spreads per fiber, for each of the three measured parameters, separating the results into the three regions and showing regional and overall averages. Average values from the previous comparisons are also shown. With the use of the housed fiber specimens, the spreads for cladding noncircularity and for core/cladding concentricity error have improved significantly for all three regions since the 1989 comparison. In North America, where the NIST SRMs are in widespread use for calibration, the average spread per fiber for mean cladding diameter measurements has improved to 0.080 μm (0.060 μm if we include only participants with calibrated test sets). The European and Pacific spreads remain higher, both at roughly 0.3 μm, although this deserves qualification.

Many of the European participants' test sets were calibrated to the United Kingdom's National Physical Laboratory (NPL), using either fiber or chrome-on-glass artifacts [9]. If we include data from only those participants, the European spread improves to 0.071 μm, which is not significantly different from the North American spread. The data of Participant 11, who calibrated with a chrome-on-glass artifact but used a different illumination scheme than for fiber measurements, were not considered calibrated. This participant also reported possible test set focusing problems for some of the comparison fibers. This participant's data showed a large systematic offset from the data of other participants with calibrated test sets. This offset is probably a result of the inconsistency in calibration procedure. This participant's data also showed a relatively large random spread, which is probably due, at least partially, to the focusing problems. If we had considered this participant's test set to be calibrated, the European spread for participants with calibrated test sets would have become 0.122 μm.

In the Pacific, only two Japanese participants' test sets were calibrated to a national standards laboratory, by use of fibers certified by the Japanese Quality Assurance Organization (JQA). Furthermore, two Pacific participants (including one of the Japanese participants with a calibrated test set, number 22) reported compatibility problems between the fiber housings and their test sets, so they could not easily and confidently measure the housed fiber specimens. Relatively large spreads in the data from these participants seem to verify these problems. We consider the data of Participant 22 to be not calibrated, since this test-set/fiber-housing incompatibility seems to more than counter the benefits of calibration. In a separate comparison, however, NIST compared three different unhoused fiber specimens with the Japanese participants and obtained a corresponding spread of roughly 0.11 μm. Table 1 shows an average spread of 0.076 μm for Pacific participants with calibrated test sets, but this is not necessarily representative, since the standard deviations were calculated using only two

data sets, from the one Pacific participant whose test set was calibrated and the NIST contact micrometer. Such numbers are probably not statistically significant and do not necessarily represent agreement among *typical* Pacific participants with calibrated test sets.

Figure 2 shows the cladding diameter results for this comparison, as a plot of offsets from NIST contact micrometer values versus participant. Up to seven points are plotted per participant, representing the seven fibers in each set of measurement specimens. The participants are grouped by region. Filled circles show participants whose gray scale test sets were calibrated by means of NIST SRMs. Filled squares show participants whose gray scale test sets were calibrated to NPL. Filled diamonds show participants whose gray scale test sets were calibrated to JQA. Open stars show the participants who reported compatibility problems between their gray scale test sets and the fiber housings, as well as the participant with focusing and calibration problems. Other gray scale data are denoted by open squares. Open triangles denote the two participants who used the image-shearing method. This graph clearly shows that those participants with test sets calibrated to one of the national standards laboratories were generally in better agreement, by as much as nearly an order of magnitude, than those whose test sets were not calibrated. Agreement generally appears to be as good for noncircular fibers as for circular. One unexplained observation, which we continue to investigate, is that most of the participants with test sets calibrated to one of the national standards laboratories had positive offsets from the NIST contact micrometer. In other words, they systematically measured slightly higher than the contact micrometer.

Two other meaningful quantities can be calculated from the statistics of these measurement offsets. For each participant, an average offset (average of the seven plotted offset values) can be calculated, as can the standard deviation of the seven offset values about that average. The average offset indicates systematic offset from the NIST contact micrometer, and, when compared to the same quantity for other participants, it indicates the extent of systematic disagreement. The magnitude of this quantity can be minimized by calibration. The second quantity, the offset standard deviation or offset spread, is a reflection of, among other things, the random uncertainty of the participant's measurements; this value would not be expected to improve with calibration. For most of the participants with noncalibrated test sets, the absolute values of the average offsets, what we call the offset magnitudes, were greater than the offset spreads. Such participants would benefit significantly from a calibration standard. All participants whose test sets were calibrated to one of the national standards laboratories had offset magnitudes of 0.16 µm or less, and all but three had less than 0.1 µm.

Table 2 shows participants' average offsets and offset spreads from this comparison. Average offset magnitude (the average of the absolute values of the participants' average offsets) and average offset spread are also given, per region, as well as overall. These numbers are reported including all participants, as well as including only those with test sets calibrated to one of the national standards laboratories. The same numbers from the 1992 TIA North American comparison are also shown. In North America the average offset magnitude has reduced from 0.114 µm in 1992, when there were no SRM calibrations, to 0.073 µm in this comparison, in which nearly all of the North American participants' test sets were calibrated by means of NIST SRMs. It reduces to 0.067 µm if we include only those so calibrated. The European average offset magnitude is somewhat higher, apparently due to the few European participants whose test sets were not calibrated to either NPL or NIST. If we include only those whose test sets were calibrated, the number reduces to 0.065 µm, which is essentially indistinguishable from the North American result. The average offset magnitude is also higher for the Pacific region, where only one participant's test set was calibrated to any national standards laboratory. That participant had an offset magnitude of 0.107 µm, much better than the regional average of 0.271 µm. The higher average offset spread in the Pacific is likely due to those test sets that had difficulty measuring the housed fiber specimens.

Figure 3 shows the results for cladding noncircularity, as a plot of offsets from NIST contact micrometer values versus participant. The NIST value, for a given fiber, is calculated from an ellipse fitted to the measured cladding diameters, taken at 45° intervals around the fiber. Given the accuracy of the NIST cladding diameter measurements and to the extent that the fibers were elliptical, these should be accurate noncircularities. Filled circles denote measurements on the four fibers that were nearly circular, while open circles denote measurements on the three noncircular fibers.

Figure 4 shows a similar plot for core/cladding concentricity error, but on this plot the offsets are from average measured values.

The measurement spreads for noncircularity and concentricity error appear to be much more nearly random than those for cladding diameter; systematic offsets between participants are not evident, except in a few cases. The noncircular fibers generally had slightly worse spreads than the circular. Table 3 shows the offset statistics, calculated using only the nearly circular fibers, for these two parameters. We know of no calibration artifacts for these two parameters, and, given the random components of most participants' offsets (evidenced by relatively large offset standard deviations), such artifacts would be only marginally useful in general. Typical specifications [1] of these parameters do not include tolerances, but rather,

maximum values.

In conclusion, this comparison shows better agreement among participants, for all three fiber geometry parameters, than did the 1989 comparison. Substantial cladding diameter disagreements seem to be systematic; this was not always the case in the 1989 comparison, in which there was more random spread in the data. Those participants whose test sets are calibrated to one of the national standards laboratories, through calibration artifacts, generally show significantly better agreement.
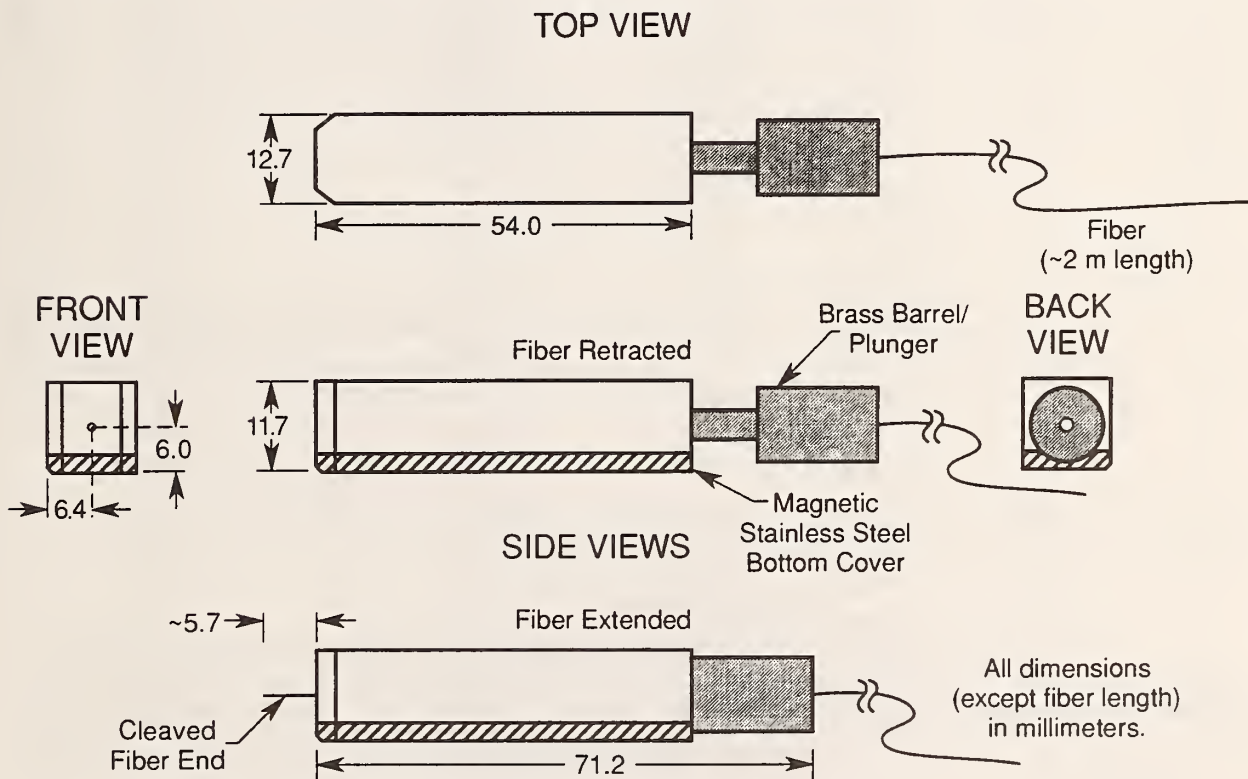
TOP VIEW

FRONT VIEW   BACK VIEW

SIDE VIEWS

Figure 1. Diagram of the NIST aluminum protective housing, used for the housed fiber measurement specimens in the interlaboratory comparison as well as for the NIST SRM calibration artifacts.

Table 1. Measurement spreads (1 standard deviation) for each fiber, for each measured parameter. Regional and overall averages are shown, as are overall averages from previous comparisons. Cladding diameter values are calculated using data from all participants and also using data from only those participants with test sets calibrated to one of the national standards laboratories.

Region	Fiber	Cladding diameter, µm		Cladding noncircularity, %	Core/cladding concentricity error, µm
		Including all participants	Including only those calibrated		
N.	A-1	0.084	0.064	0.055	0.069
	A-2	0.082	0.060	0.051	0.031
A	A-3	0.079	0.057	0.056	0.091
m	A-4	0.072	0.057	0.056	0.079
e	A-5	0.075	0.054	0.047	0.072
r	A-6	0.082	0.066	0.038	0.038
i	A-7	0.083	0.062	0.047	0.064
c					
a	**Average**	**0.080**	**0.060**	**0.050**	**0.064**
	E-1	0.273	0.062[a]	0.052	0.097
	E-2	0.329	0.088[a]	0.032	0.161
E	E-3	0.318	0.039[a]	0.149	0.085
u	E-4	0.286	0.077[a]	0.073	0.105
r	E-5	0.263	0.067[a]	0.153	0.126
o	E-6	0.308	0.076[a]	0.213	0.123
p	E-7	0.271	0.085[a]	0.063	0.090
e					
	Average	**0.293**	**0.071[a]**	**0.105**	**0.112**
	P-1	0.266	0.088[b]	0.156	0.057
P	P-2	0.304	0.079[b]	0.069	0.033
a	P-3	0.304	0.083[b]	0.081	0.093
c	P-4	0.288	0.062[b]	0.092	0.080
i	P-5	0.346	0.046[b]	0.122	0.056
f	P-6	0.310	0.073[b]	0.131	0.082
i	P-7	0.297	0.098[b]	0.135	0.055
c					
	Average	**0.302**	**0.076[b]**	**0.112**	**0.065**
Overall average		**0.225**	**0.069**	**0.089**	**0.080**
PREVIOUS COMPARISONS					
'89 CCITT (International)		0.38		0.27	0.17
'92 TIA (N. American)		0.15		0.05	0.04

[a]Does not include data from one participant (number 11) who reported probable test set focusing problems. Also, their test set was calibrated, but under different illumination conditions than for fiber measurements.

[b]Does not include data from one participant (number 22) whose test set was calibrated but had compatibility problems with the fiber housings. Therefore, these standard deviations are calculated from only one calibrated Pacific test set and NIST contact micrometer values, so they are not necessarily representative of a typical calibrated Pacific test set.
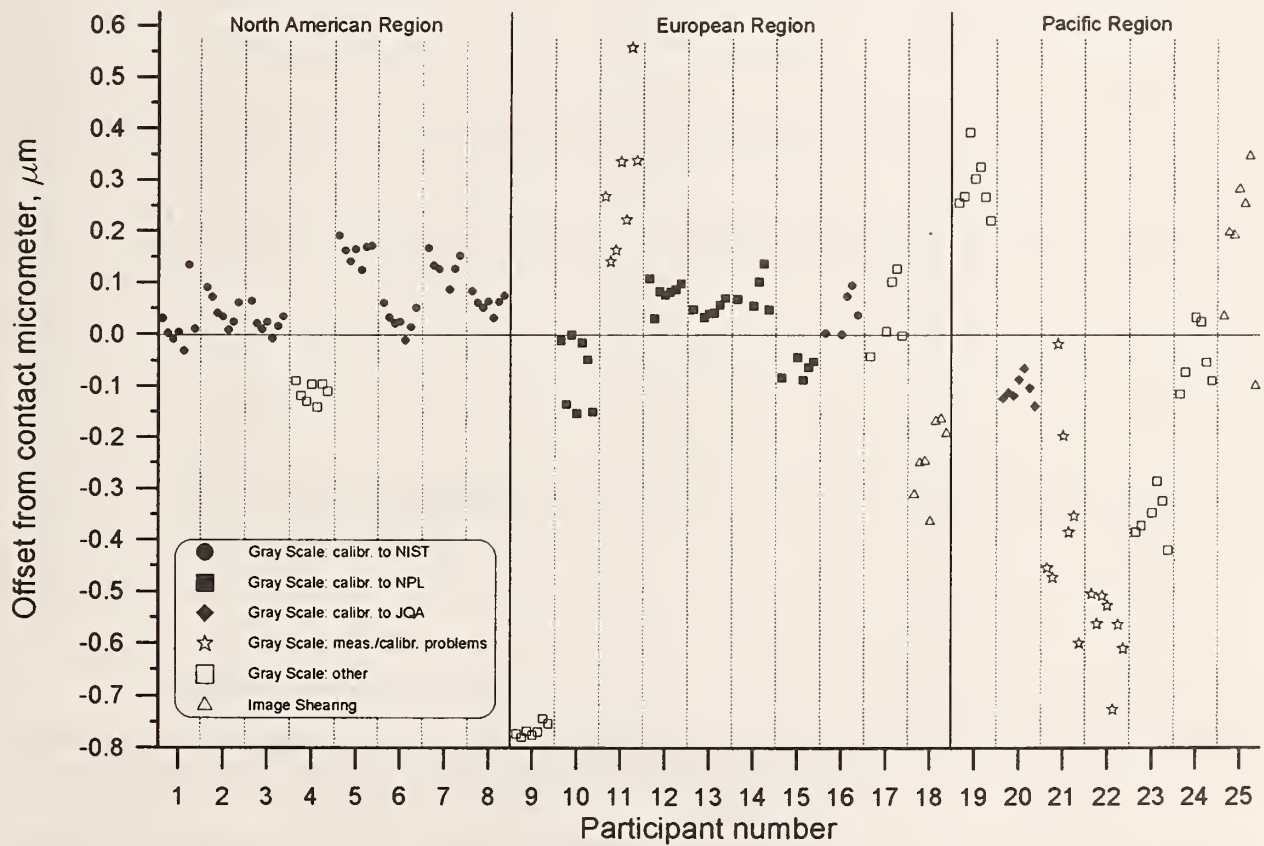
Figure 2. Offsets of participants' cladding diameter measurements from NIST contact micrometer values. Up to seven points plotted, for each participant, represent the seven fibers in the measurement samples.

9

Table 2. Statistics for participants' cladding diameter offsets from NIST contact micrometer. Regional and overall averages are given for all participants and for only those with test sets calibrated to one of the national standards laboratories. Corresponding results from previous comparison are also shown.

Region	Participant	Average offset, μm	Standard deviation of offsets, μm
N.	1[a]	+0.020	0.054
	2[a]	+0.047	0.029
A	3[a]	+0.023	0.022
m	4	−0.111	0.019
e	5[a]	+0.160	0.022
r			
i	6[a]	+0.027	0.024
c	7[a]	+0.131	0.027
a	8[a]	+0.061	0.016
	9	−0.765	0.013
	10[b]	−0.073	0.070
E	11[c]	+0.289	0.141
u	12[b]	+0.081	0.024
r	13[b]	+0.048	0.013
o	14[b]	+0.082	0.037
p	15[b]	−0.066	0.019
e	16[a]	+0.041	0.042
	17	+0.038	0.073
	18	−0.242	0.075
P	19	+0.290	0.056
a	20[d]	−0.107	0.025
c	21	−0.354	0.193
i	22[e]	−0.571	0.077
f	23	−0.355	0.047
i	24	−0.045	0.061
c	25	+0.173	0.154

Region	Average offset magnitude,[f] μm		Average offset spread,[g] μm	
	Including all participants	Including only those calibrated	Including all participants	Including only those calibrated
N. America	0.073	0.067	0.027	0.028
Europe	0.173	0.065	0.051	0.034
Pacific	0.271	0.107	0.088	0.025
Overall	**0.168**	**0.069**	**0.053**	**0.030**
PREVIOUS COMPARISON				
'92 TIA (N. American)	0.114		0.032	

[a]Calibrated to NIST.   [b]Calibrated to NPL.   [d]Calibrated to JQA.

[c]Not considered calibrated. Calibration to NPL done with different illumination than for fiber measurements. Also reported probable focusing problems with test set, for some fibers.

[e]Not considered calibrated. Calibration to JQA countered by incompatibility between test set and fiber housings.

[f]Average of absolute values of participants' average offsets.

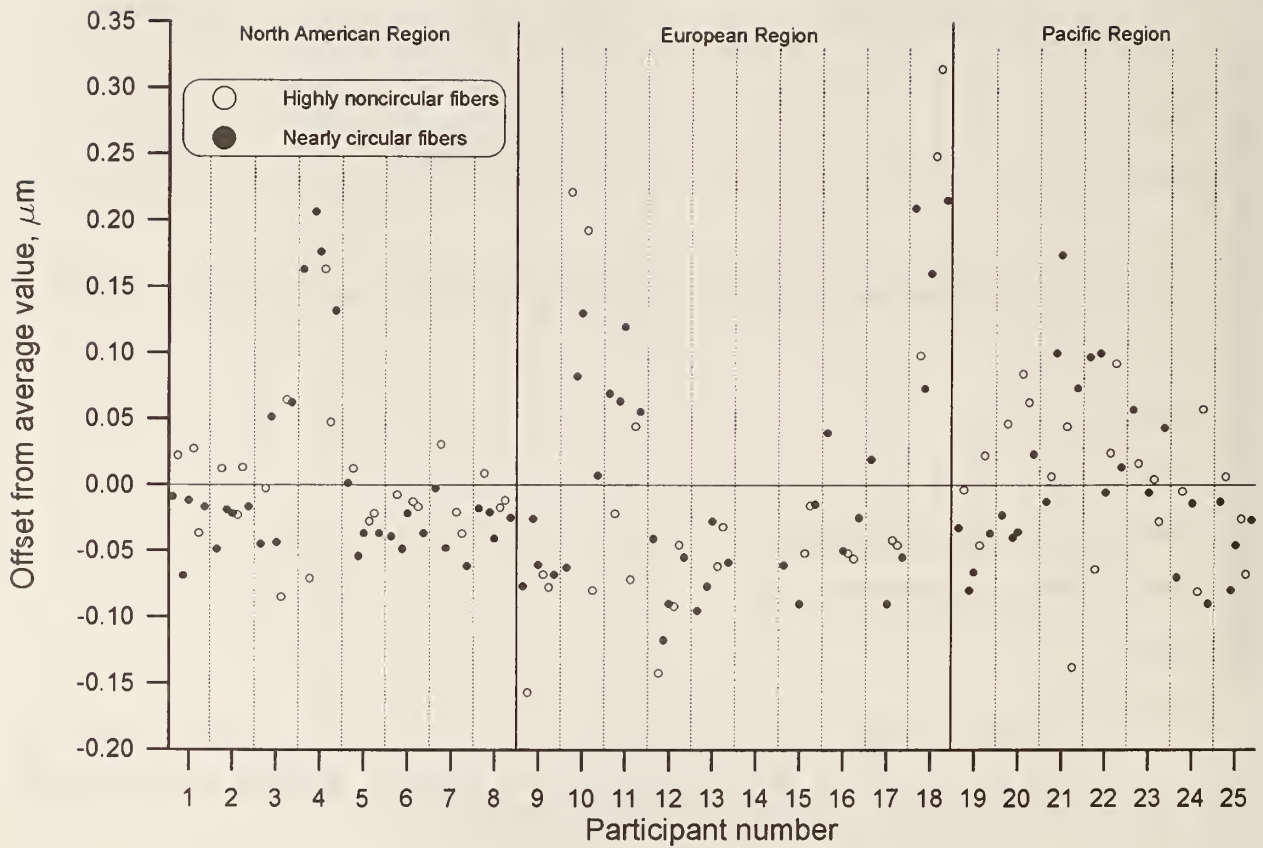[g]Average of participants' offset standard deviations.

Figure 3. Offsets of participants' cladding noncircularity measurements from NIST contact micrometer fitted values. The NIST value, for a given fiber, is calculated from an ellipse fitted to measured cladding diameter values. Up to seven points plotted, for each participant, represent the seven fibers in the measurement samples. Filled symbols denote nearly circular fibers (less than 0.1 percent noncircularity), while open symbols denote more highly noncircular fibers (up to 1.5 percent noncircularity).

Figure 4. Offsets of participants' core/cladding concentricity error measurements from average values. Up to seven points plotted, for each participant, represent the seven fibers in the measurement samples. Filled symbols denote nearly circular fibers (less than 0.1 percent noncircularity), while open symbols denote more highly noncircular fibers (up to 1.5 percent noncircularity).

Table 3. Statistics for participants' cladding noncircularity offsets from NIST values and core/cladding concentricity error offsets from average values, including only nearly circular (noncircularity less than 0.1 percent) fibers.

Region	Participant	Cladding noncircularity offsets from NIST contact micrometer values (nearly circular fibers only)		Core/cladding concentricity error offsets from average values (nearly circular fibers only)	
		Average offset, %	Standard deviation of offsets, %	Average offset, μm	Standard deviation of offsets, μm
N. America	1	+0.150	0.019	−0.027	0.028
	2	−0.003	0.023	−0.027	0.015
	3	+0.054	0.027	+0.006	0.059
	4	+0.040	0.010	+0.169	0.031
	5	−0.002	0.005	−0.032	0.023
	6	−0.001	0.005	−0.037	0.011
	7	+0.061	0.048	−0.028	0.031
	8	+0.050	0.004	−0.026	0.010
Europe	9	+0.005	0.012	−0.058	0.022
	10	+0.140	0.125	+0.039	0.085
	11	+0.166	0.110	+0.077	0.029
	12	+0.009	0.032	−0.076	0.034
	13	0.000	0.021	−0.065	0.028
	14	0.000	0.013		
	15	+0.003	0.008	−0.042	0.041
	16	+0.013	0.010	−0.009	0.038
	17	+0.050	0.035	−0.032	0.050
	18	+0.147	0.071	+0.164	0.066
Pacific	19	+0.043	0.017	−0.054	0.023
	20	−0.004	0.031	−0.019	0.029
	21	+0.153	0.202	+0.084	0.077
	22	+0.283	0.096	+0.051	0.055
	23	+0.052	0.056	+0.024	0.031
	24	+0.031	0.033	−0.044	0.043
	25	+0.066	0.053	−0.041	0.029

Region	Average offset magnitude,[a] μm	Average offset spread,[b] μm	Average offset magnitude,[a] μm	Average offset spread,[b] μm
N. America	0.045	0.018	0.044	0.026
Europe	0.053	0.044	0.062	0.044
Pacific	0.090	0.070	0.045	0.041
Overall	**0.061**	**0.043**	**0.051**	**0.037**

[a]Average of absolute values of participants' average offsets. [b]Average of participants' offset standard deviations.

3. Fiber Coating Geometry

NIST coordinated an interlaboratory comparison, among TIA members, of measurements of diameter, concentricity (coating/cladding concentricity error), noncircularity, and wall thickness of fiber primary coatings. Standard telecommunications fibers usually have two layers (inner and outer) of acrylate coatings, with the diameter of the outer layer nominally 250 μm. The goal of this comparison was to check the interlaboratory agreement among participants using different methods and among those using any given method.

Six fibers, designated *A* through *F*, were measured. Three (*B*, *C*, and *D*) were standard dual-coated fibers with nominally 250 μm outer coating diameter. One (*A*) was an older single-coated fiber. Another (*E*) was hermetically coated; that is, a very thin opaque hermetic layer was applied to the fiber for extra strength and protection, and then the coated fiber was covered with a nominally 170 μm acrylate coating. The final fiber (*F*) was a "fat" (nominally 500 μm outer coating diameter) dual-coated fiber. Each participant measured different specimens of these fibers. It was not practical to send the same specimens around serially, since, as part of measurement, the fibers are immersed in index-matching oils which may be absorbed by the coatings over time and may change them. To minimize the effects of longitudinal nonuniformities, each participant received three specimens of each fiber, cut from different locations on the spools. Averages of measurements on each set of three specimens were used in calculating the results presented here. Most of the measurement methods required knowledge of the indexes of refraction of the coating layers of the fibers. Three laboratories measured these indexes, and consensus values were provided to the participants.

Eight laboratories made measurements, submitting a total of ten data sets. The data sets were arranged by measurement method and assigned participant numbers, 1 through 10. Four measurement methods, represented by TIA Fiber Optic Test Procedures (FOTPs), were used. Participants 1 through 5 used FOTP-173 [10], a side-view video method, in which measurements are under manual control. Participants 6 through 8 used FOTP-163 [11], an automated extension of FOTP-173, in which a fiber is rotated through a user-defined number of angular orientations and a computer fits the data from each layer of coating and computes the geometrical parameters. Participant 9 used FOTP-119 [12], which is an end-view automated video method, in which edges and layer boundaries are located by gray scale analysis, much as in the fiber (glass) geometry gray scale method [7]. For outer layer diameter measurements only, Participant 10 used a Michelson interferometric microscope, essentially following FOTP-93 [13], which describes this method for fiber cladding diameter measurements; this is not a TIA-approved method for coating diameter measurements.

Table 4 shows the measurement spreads, per fiber, for each of the coating geometry parameters. Average values, calculated from measurements of only the standard 250 μm dual-coated fibers, are also shown. The only coating geometry parameter to currently have a TIA-specified tolerance is outer layer diameter. The tolerance required is ±10 μm [1]. To comfortably meet this tolerance, agreement and, hence, accuracy on the order of ±1 μm are desired. The average spread for outer layer diameter measurements in this comparison was ±1.6 μm (1 standard deviation) and is possibly sufficient to support the desired tolerance. The average spread for inner layer diameter measurements was considerably larger, 3.19 μm. A major difference between outer layer and inner layer spreads also occurred for noncircularity measurements; only two participants measured inner layer noncircularity, however, so the average spread may not be typical. Conversely, for minimum and maximum wall thickness measurements, the average spreads for the inner layers were smaller than for the outer layers, with eight participants measuring both. The average spreads for minimum and maximum wall thickness measurements on the combined (inner and outer) layers were even slightly smaller than for the inner layer alone, but only four participants measured the combined layers.

Figure 5 is a plot of the offsets of outer layer coating diameter measurements from average values versus participant. Up to six points plotted per participant represent the six fibers in the measurement sample. Filled points represent measurements on the standard 250 μm dual-coated fibers. Open symbols denote the nonstandard fibers, as defined in the graph legend. For the standard fibers, there are definite systematic components to the offsets of nearly all participants. Participant 8, in particular, shows a large systematic offset. These could be minimized through accurate calibration. NIST plans to develop an SRM calibration artifact for coating outside diameter, which should be available some time in 1996. The random components of the participants' offsets, which are related to the precision of the test sets and are shown on the graph by the degree of clumping of given participants' offset data, range from very small (Participants 5 and 8) to fairly large (Participants 1 and 3).

Figure 6 is the same type of plot for inner layer diameter. Offsets are much larger in general, and many participants show large systematic and/or random components to their offsets. Participant 5 was the only one to report inner layer diameters for the hermetically coated fiber.

The average offset and the standard deviation of the offsets about that average, for each participant's outer and inner layer diameter measurements, are shown in table 5. The outer layer average offset magnitude is considerably larger than the average offset spread, so

calibration should improve interlaboratory agreement. Accurate calibration would reduce the average offset magnitude and allow the overall average spread (1.6 μm in this comparison, from table 4) to approach a value on the order of the average offset spread (0.5 μm) seen here. In this case, the industry could confidently meet the desired tolerance of ±10 μm. The offset statistics for inner layer diameter also show an average offset magnitude larger than the average offset spread, so a calibration artifact that included inner layer diameter could be useful if the industry were to ever desire an inner layer diameter tolerance tighter than that supported by the interlaboratory agreement in this comparison.

For concentricity measurements, outer layer offsets from average are shown in figure 7 and inner layer in figure 8. Similar vertical scales on these graphs show that concentricity measurements on the outer and inner coating layers had very similar precision. There do not appear to be large systematic components to participants' offsets in general. This is verified in table 6, which shows the offset statistics for outer and inner layer concentricity measurements. The outer and inner layer average offset magnitudes are smaller, for concentricity, than the average offset spreads, so a calibration artifact for concentricity would not improve agreement significantly. In other words, interlaboratory agreement for concentricity measurements is limited by the precision of the instruments.

Similar offset plots for noncircularity measurements are shown for outer coating layer in figure 9 and for inner layer in figure 10. There are not enough inner layer noncircularity data to draw definite conclusions, except that the disagreement between the two participants making inner layer measurements was considerably greater than that among several participants making outer layer measurements. Noncircularity offset statistics are shown in table 7. For outer layer measurements, the average offset magnitude and average offset spread are roughly equal, so a calibration artifact that included outer layer noncircularity could improve interlaboratory agreement, but only slightly.

Diameter, concentricity, and noncircularity are the parameters calculated and reported from the TIA FOTPs. To calculate concentricity, however, certain coating wall thicknesses are needed. In this comparison, participants measured the minimum and maximum wall thicknesses of both the outer and inner coating layers, as well as of the combined (inner and outer layers) coating. These data were an additional test of participants' ability to measure edges or boundaries between the two layers of coating and between the fiber cladding and the inner coating layer.

Figure 11 is a plot of offsets from average values for measurements of the minimum wall thicknesses of the outer layers. Figure 12 is the same, for maximum wall thickness. Table 8 shows the offset statistics for these graphs. There are definite systematic components to participants' offsets, and they are very similar for both minimum and maximum wall thickness measurements. Figure 13 is the same type of plot for the minimum and figure 14 for the maximum wall thicknesses of the inner layers. Table 9 shows the offset statistics for these two graphs. Agreement was better on the inner layer measurements, and the systematic nature of participants' offsets was much less pronounced than for the outer layer measurements. For each participant, the systematic component of inner layer measurement offsets did not tend to correlate well with that of the outer layer offsets.

Figure 15 is a similar plot for minimum wall thickness of the combined layers. Figure 16 is the same, for maximum combined wall thickness. Only four participants made these measurements, but several results are clear. The overall agreement is better than for the outer layer measurements and comparable to that for the inner layer measurements. There are obvious systematic components to the participants' offsets. Offset statistics are shown in table 10. The average offset spreads of the measurements on the combined layers are considerably smaller than those of either the outer or inner layers alone. This indicates that the precision on wall thickness measurements on the combined layers is better than for similar measurements on either layer individually.

For the coating comparison, there was good overall agreement among measurement methods. There were no obvious systematic differences between methods for any of the measured parameters. For FOTP-163 and FOTP-173, data from one method were in all cases almost completely contained within the spread of data from the other method. For FOTP-119 (and FOTP-93 for outer layer diameter only), there was only one participant, so general conclusions are difficult. However, for all parameters, even though some systematic offsets occurred, the FOTP-119 (and FOTP-93) data were generally bracketed within the spread from the other methods.

Finally, a similar comparison of coating diameter, concentricity, and noncircularity measurements was done in Europe. Three fibers from the TIA/NIST comparison were provided to the European coordinator. At the completion of both comparisons, results for the common fibers were exchanged. European participants used side-viewing and end-viewing methods. Some of their methods conformed to the TIA FOTPs, while others did not. Measurement results from the European comparison were contained within the TIA/NIST measurement spreads reported here.

Table 4. Measurement spreads (1 standard deviation) for all measurements made on each fiber, for all fiber coating parameters. Averages calculated using only the standard, nominally 250 μm, dual-coated fibers (specimens B, C, and D).

Measured parameter	Fiber specimen						Average value (for standard 250 μm dual-coated fibers, B, C, and D)
	A[a]	B	C	D	E[b]	F[c]	
Outer layer diameter, μm	1.64	1.54	1.64	1.63	1.75	2.90	**1.60**
Inner layer diameter, μm		2.80	3.81	2.97		6.40	**3.19**
Outer layer concentricity, μm	0.32	0.80	0.71	0.79	0.22	1.71	**0.77**
Inner layer concentricity, μm		1.13	0.22	0.75		1.06	**0.70**
Outer layer noncircularity, %	0.10	0.27	0.35	0.25	0.20	0.14	**0.29**
Inner layer noncircularity, %		1.22	0.36	1.75			**1.11**
Outer layer minimum wall thickness, μm	1.10	1.85	2.11	1.17	4.66	2.37	**1.71**
Outer layer maximum wall thickness, μm	1.17	1.74	2.42	1.25	4.61	4.03	**1.80**
Inner layer minimum wall thickness, μm		1.31	1.19	1.24		2.34	**1.25**
Inner layer maximum wall thickness, μm		1.28	1.27	0.85		1.93	**1.13**
Combined layers minimum wall thickness, μm		0.98	1.03	0.95		2.87	**0.99**
Combined layers maximum wall thickness, μm		1.37	1.06	0.84		1.67	**1.09**

[a]Single-coated fiber.   [b]Hermetically coated fiber.   [c]"Fat" (500 μm coating) fiber.
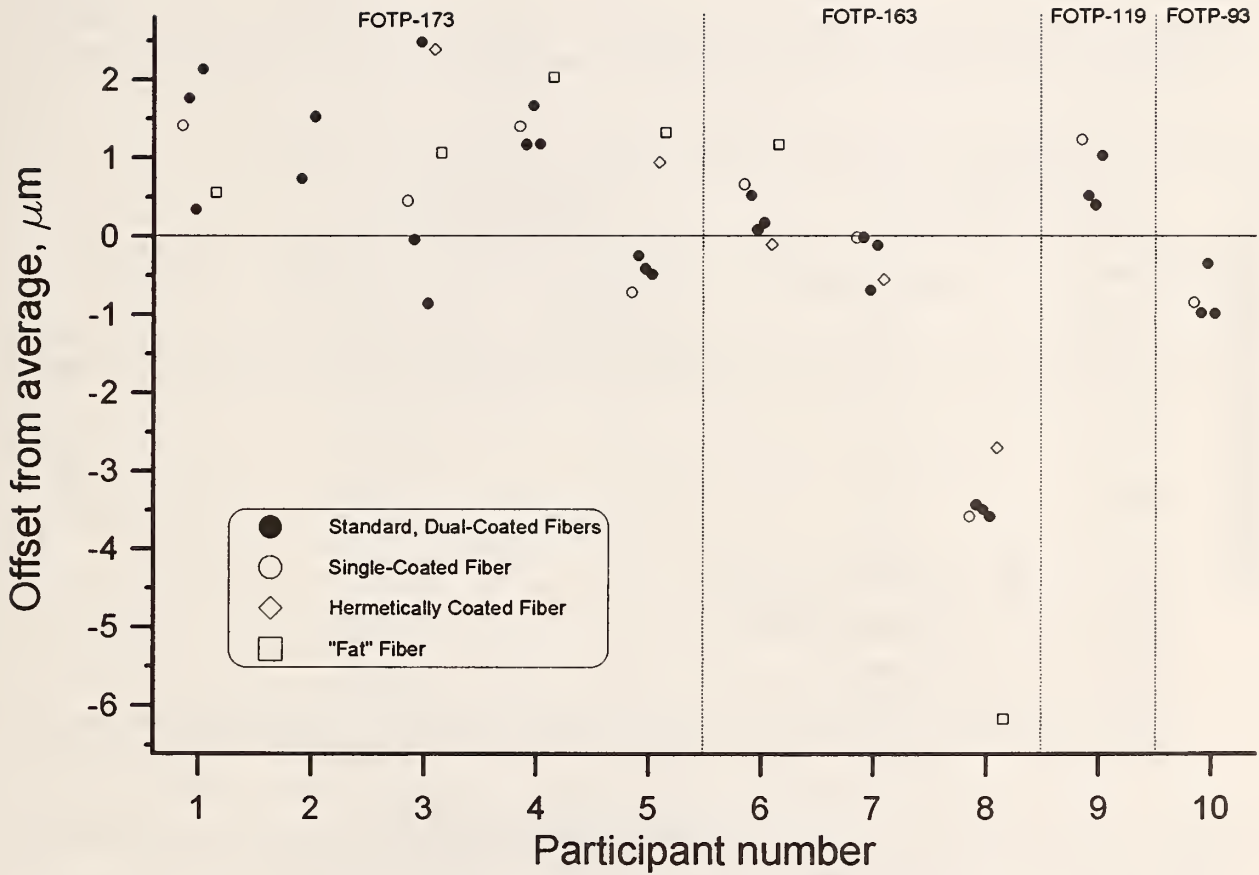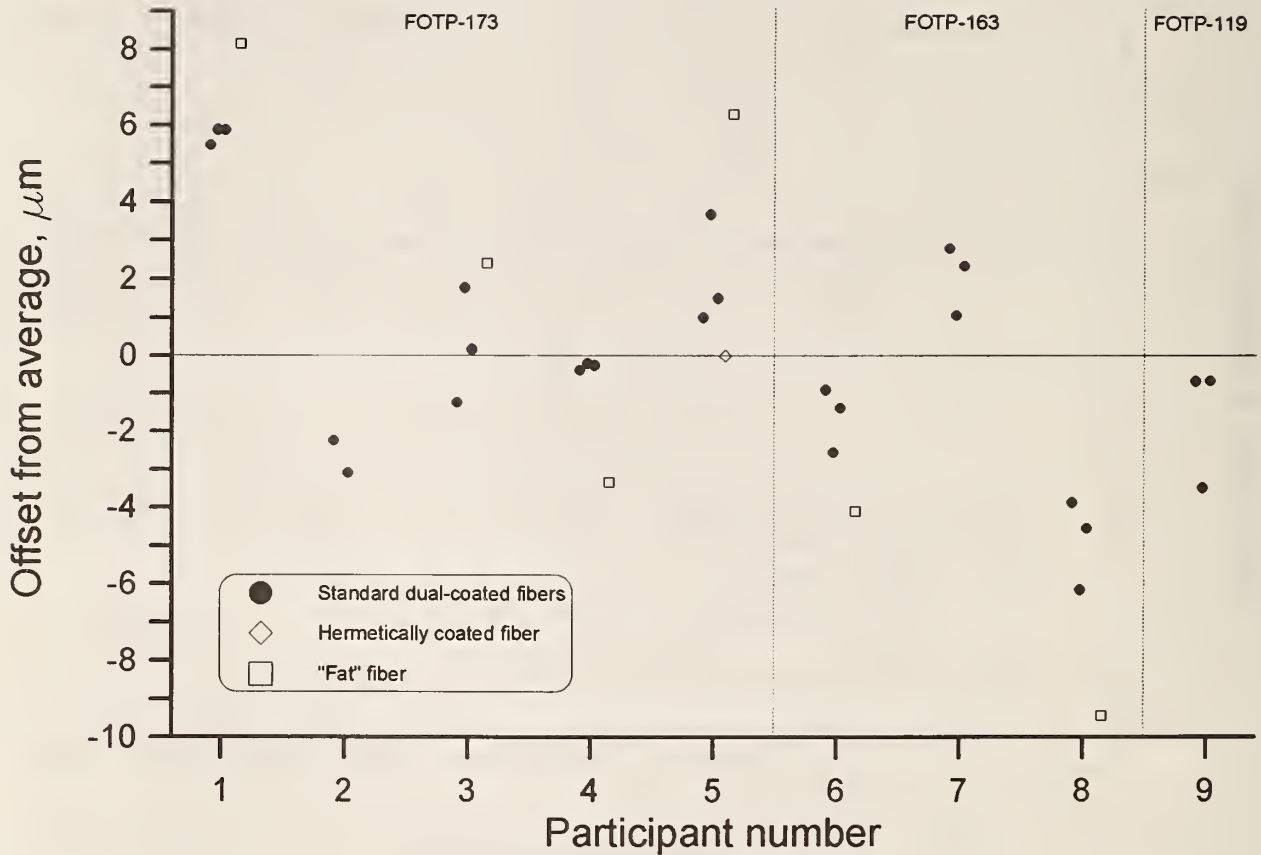
Figure 5. Offsets of participants' fiber coating outer layer diameter measurements from average values. Up to six points plotted, for each participant, represent the six fibers in the measurement sample. Filled symbols denote standard, nominally 250 μm, dual-coated fibers. Open symbols denote non-standard fibers: single-coated, hermetically coated, and "fat" (nominally 500 μm). Participants are grouped according to their measurement methods, identified by TIA Fiber Optic Test Procedure (FOTP) numbers.
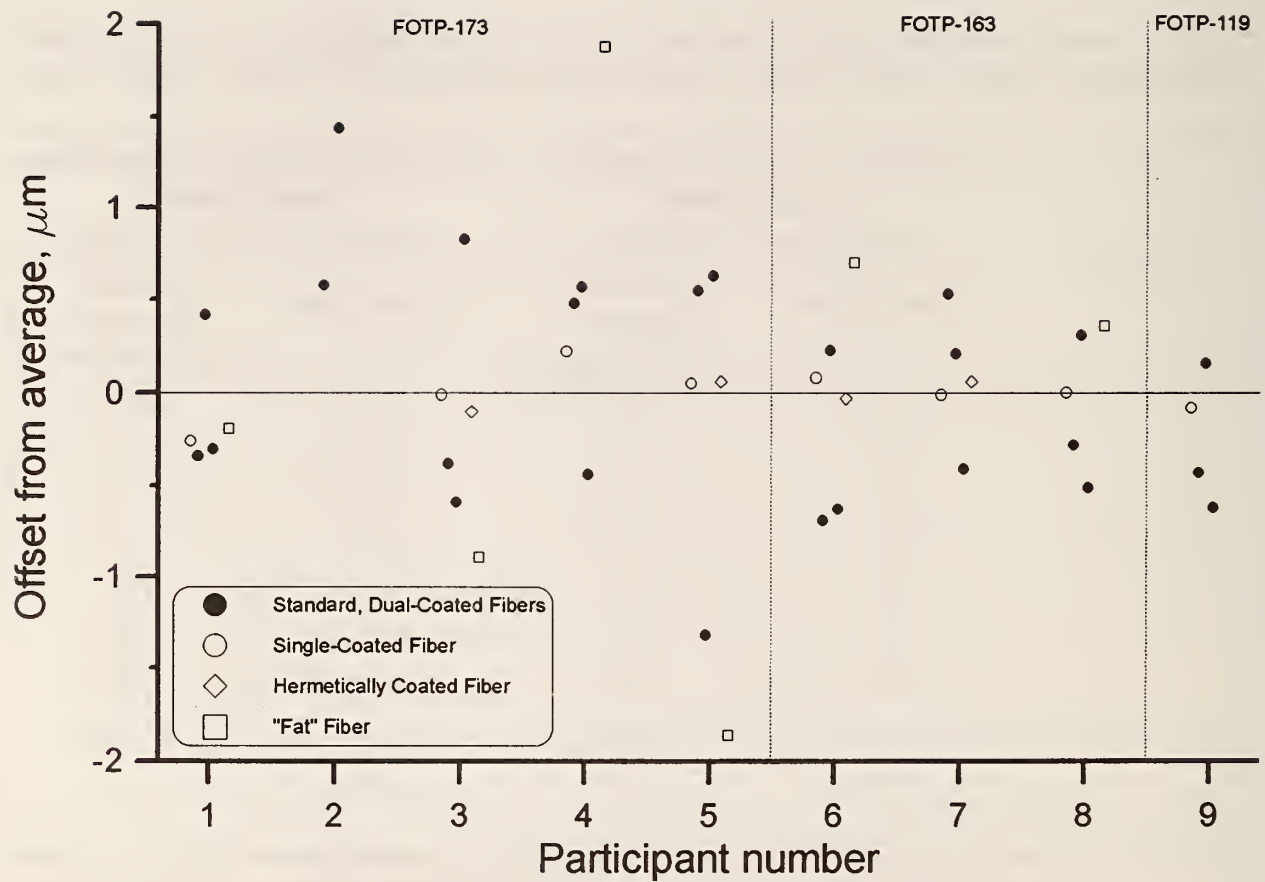
Figure 6. Offsets of participants' fiber coating inner layer diameter measurements from average values. Up to five points plotted, for each participant, represent those of the six fibers in the measurement sample for which this parameter exists. Filled symbols denote standard 250 µm dual-coated fibers. Open symbols denote non-standard fibers: hermetically coated and "fat" (nominally 500 µm). Participants are grouped according to their measurement methods, identified by TIA Fiber Optic Test Procedure (FOTP) numbers.
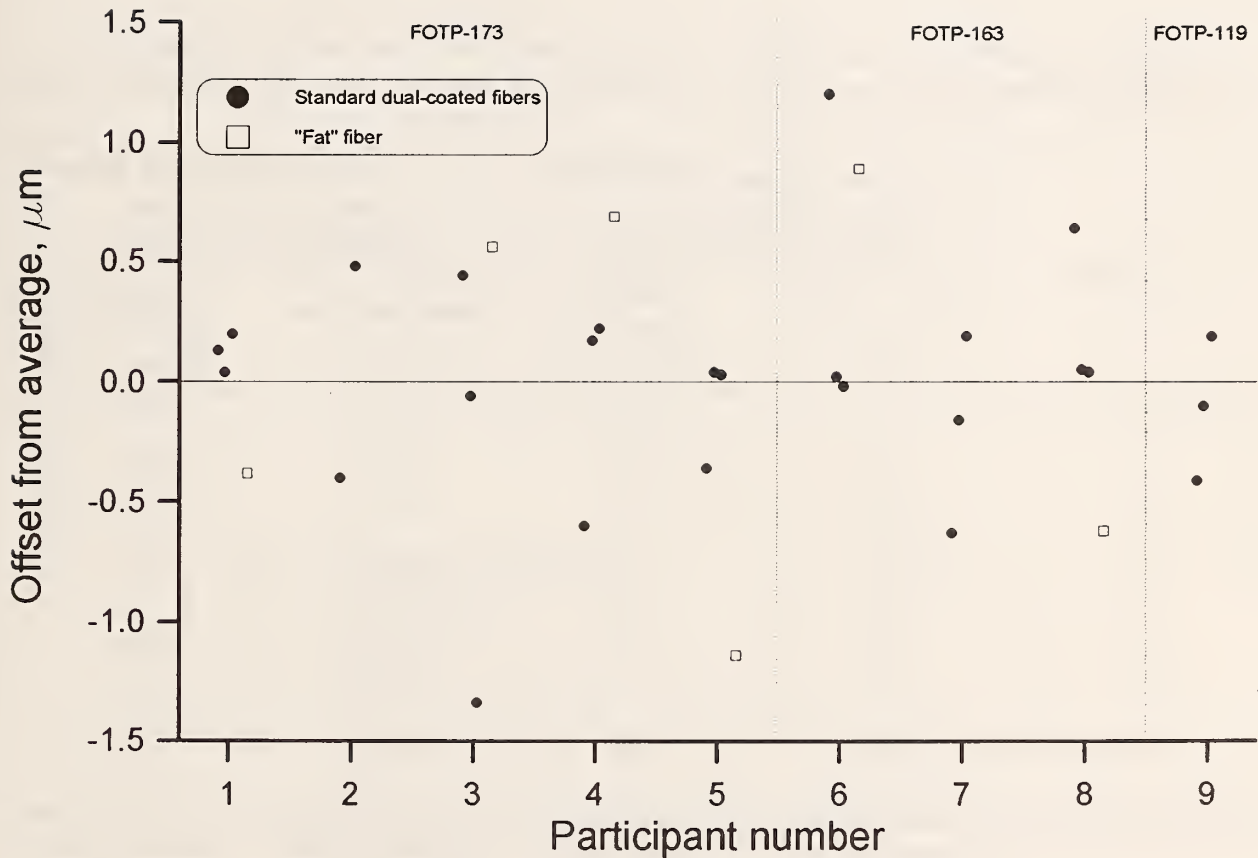
Table 5. Statistics for participants' outer and inner layer fiber coating diameter measurement offsets from average values, including only standard, nominally 250 μm, dual-coated fibers.

Participant	Outer layer diameter offsets from average values (standard dual-coated fibers)		Inner layer diameter offsets from average values (standard dual-coated fibers)	
	Average offset, μm	Standard deviation of offsets, μm	Average offset, μm	Standard deviation of offsets, μm
1	+1.41	0.95	+5.75	0.23
2	+1.14	0.55	−2.67	0.59
3	+0.52	1.74	+0.24	1.50
4	+1.34	0.28	−0.27	0.09
5	−0.39	0.12	+2.06	1.42
6	+0.26	0.24	−1.60	0.84
7	−0.28	0.36	+2.07	0.90
8	−3.50	0.08	−4.86	1.18
9	+0.65	0.33	−1.61	1.63
10	−0.78	0.37		
	Average offset magnitude,[a] μm	Average offset spread,[b] μm	Average offset magnitude,[a] μm	Average offset spread,[b] μm
	1.03	**0.50**	**2.35**	**0.93**

[a]Average of absolute values of participants' average offsets.

[b]Average of participants' offset standard deviations.

21

Figure 7. Offsets of participants' fiber coating outer layer concentricity measurements from average values. Up to six points plotted, for each participant, represent the six fibers in the measurement sample. Filled symbols denote standard 250 μm dual-coated fibers. Open symbols denote non-standard fibers: single-coated, hermetically coated, and "fat" (nominally 500 μm). Participants are grouped according to their measurement methods, identified by TIA Fiber Optic Test Procedure (FOTP) numbers.
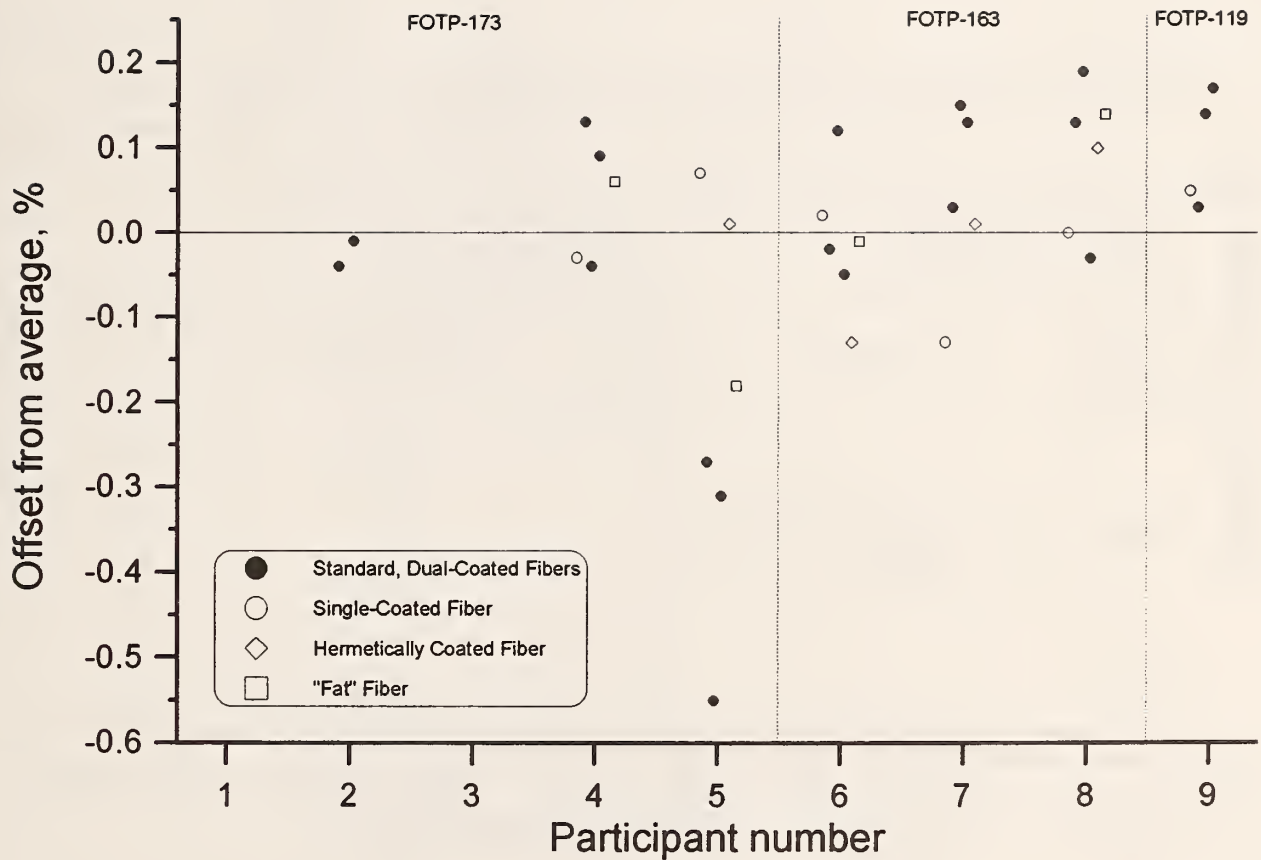
Figure 8. Offsets of participants' fiber coating inner layer concentricity measurements from average values. Up to four points plotted, for each participant, represent those of the six fibers in the measurement sample for which measurements of this parameter were made. Filled symbols denote standard 250 μm dual-coated fibers. Open symbols denote a non-standard, "fat" (nominally 500 μm) fiber. Participants are grouped according to their measurement methods, identified by TIA Fiber Optic Test Procedure (FOTP) numbers.
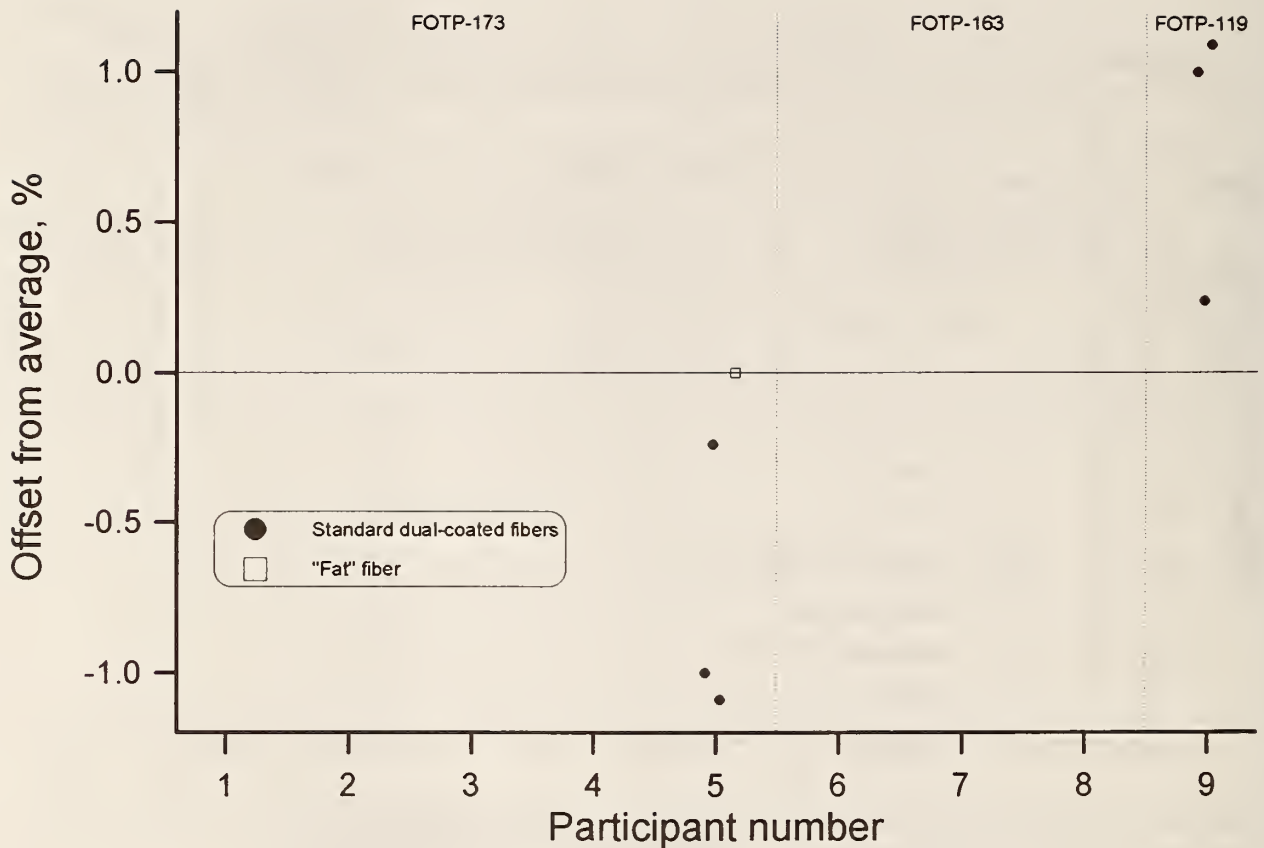
Table 6. Statistics for participants' outer and inner layer fiber coating concentricity measurement offsets from average values, including only standard 250 μm dual-coated fibers.

Participant	Outer layer concentricity offsets from average values (standard dual-coated fibers)		Inner layer concentricity offsets from average values (standard dual-coated fibers)	
	Average offset, μm	Standard deviation of offsets, μm	Average offset, μm	Standard deviation of offsets, μm
1	−0.07	0.43	+0.12	0.08
2	+1.01	0.61	+0.04	0.63
3	−0.05	0.77	−0.32	0.92
4	+0.21	0.56	−0.07	0.46
5	−0.05	1.10	−0.10	0.23
6	−0.36	0.51	+0.40	0.69
7	+0.11	0.47	−0.20	0.41
8	−0.16	0.42	+0.24	0.35
9	−0.30	0.41	−0.11	0.30
	Average offset magnitude,[a] μm	Average offset spread,[b] μm	Average offset magnitude,[a] μm	Average offset spread,[b] μm
	0.26	0.59	0.18	0.45

[a]Average of absolute values of participants' average offsets.

[b]Average of participants' offset standard deviations.

Figure 9. Offsets of participants' fiber coating outer layer noncircularity measurements from average values. Up to six points plotted, for each participant, represent the six fibers in the measurement sample. Filled symbols denote standard 250 μm dual-coated fibers. Open symbols denote non-standard fibers: single-coated, hermetically coated, and "fat" (nominally 500 μm). Participants are grouped according to their measurement methods, identified by TIA Fiber Optic Test Procedure (FOTP) numbers.
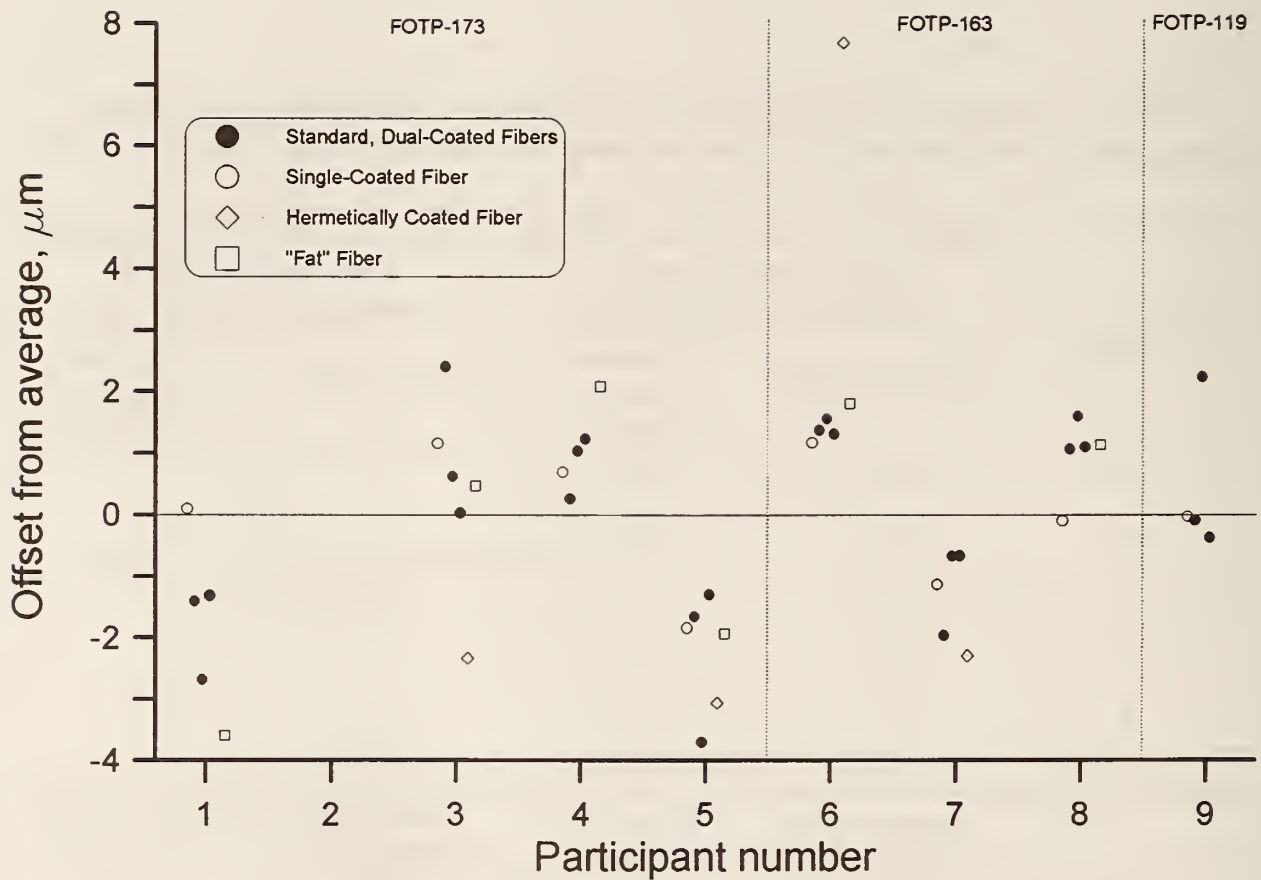
Figure 10. Offsets of participants' fiber coating inner layer noncircularity measurements from average values. Up to four points plotted, for each participant, represent those of the six fibers in the measurement sample for which measurements of this parameter were made. Filled symbols denote standard 250 μm dual-coated fibers. Open symbols denote a non-standard, "fat" (nominally 500 μm) fiber. Participants are grouped according to their measurement methods, identified by TIA Fiber Optic Test Procedure (FOTP) numbers.

Table 7. Statistics for participants' outer and inner layer fiber coating noncircularity measurement offsets from average values, including only standard 250 µm dual-coated fibers.

Participant	Outer layer noncircularity offsets from average values (standard dual-coated fibers)		Inner layer noncircularity offsets from average values (standard dual-coated fibers)	
	Average offset, %	Standard deviation of offsets, %	Average offset, %	Standard deviation of offsets, %
2	−0.02	0.02		
4	+0.06	0.09		
5	−0.38	0.15	−0.78	0.47
6	+0.02	0.09		
7	+0.10	0.06		
8	+0.10	0.12		
9	+0.12	0.07	+0.78	0.47
	Average offset magnitude,[a] %	Average offset spread,[b] %	Average offset magnitude,[a] %	Average offset spread,[b] %
	0.11	**0.09**	**0.78**	**0.47**

[a]Average of absolute valued of participants' average offsets.

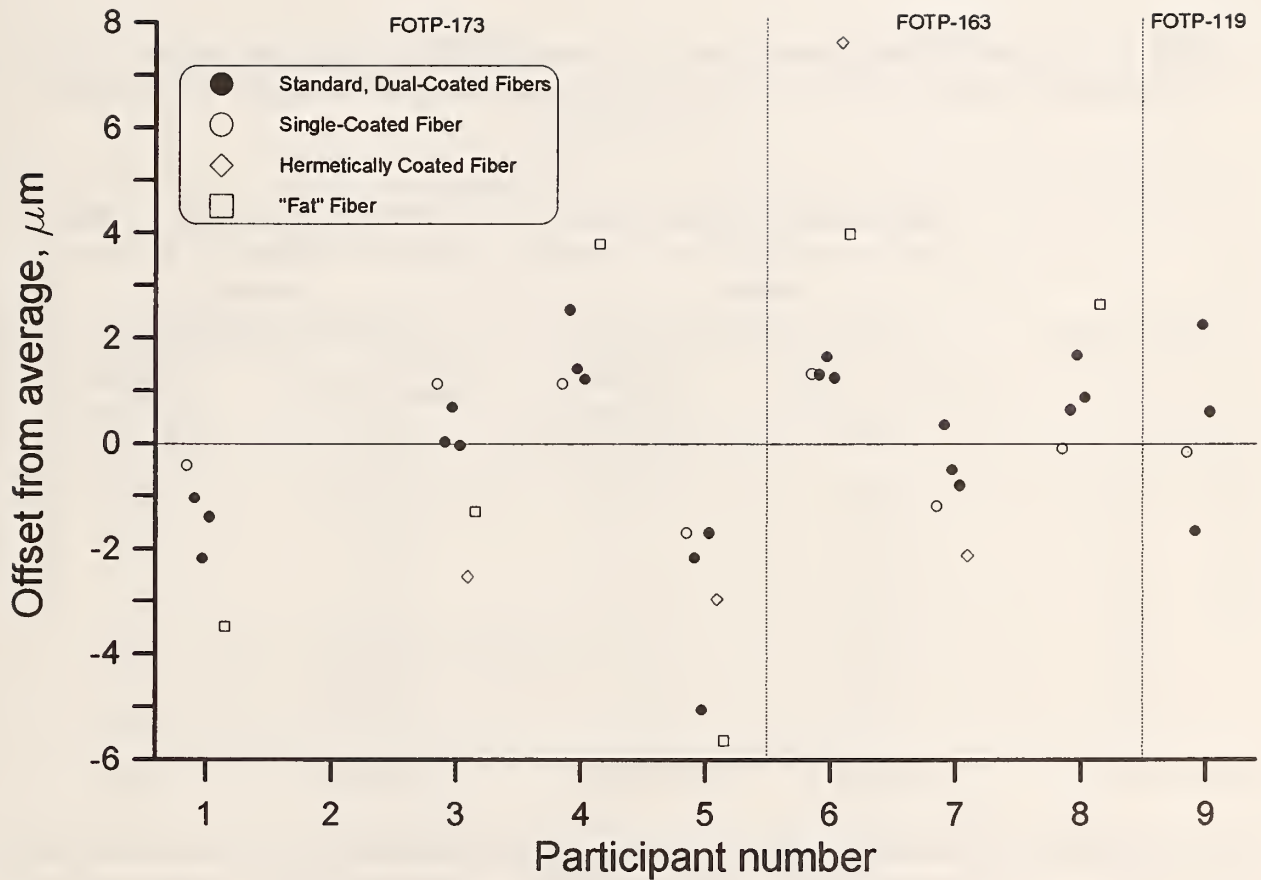[b]Average of participants' offset standard deviations.

Figure 11. Offsets of participants' fiber coating outer layer minimum wall thickness measurements from average values. Up to six points plotted, for each participant, represent the six fibers in the measurement sample. Filled symbols denote standard 250 μm dual-coated fibers. Open symbols denote non-standard fibers: single-coated, hermetically coated, and "fat" (nominally 500 μm). Participants are grouped according to their measurement methods, identified by TIA Fiber Optic Test Procedure (FOTP) numbers.
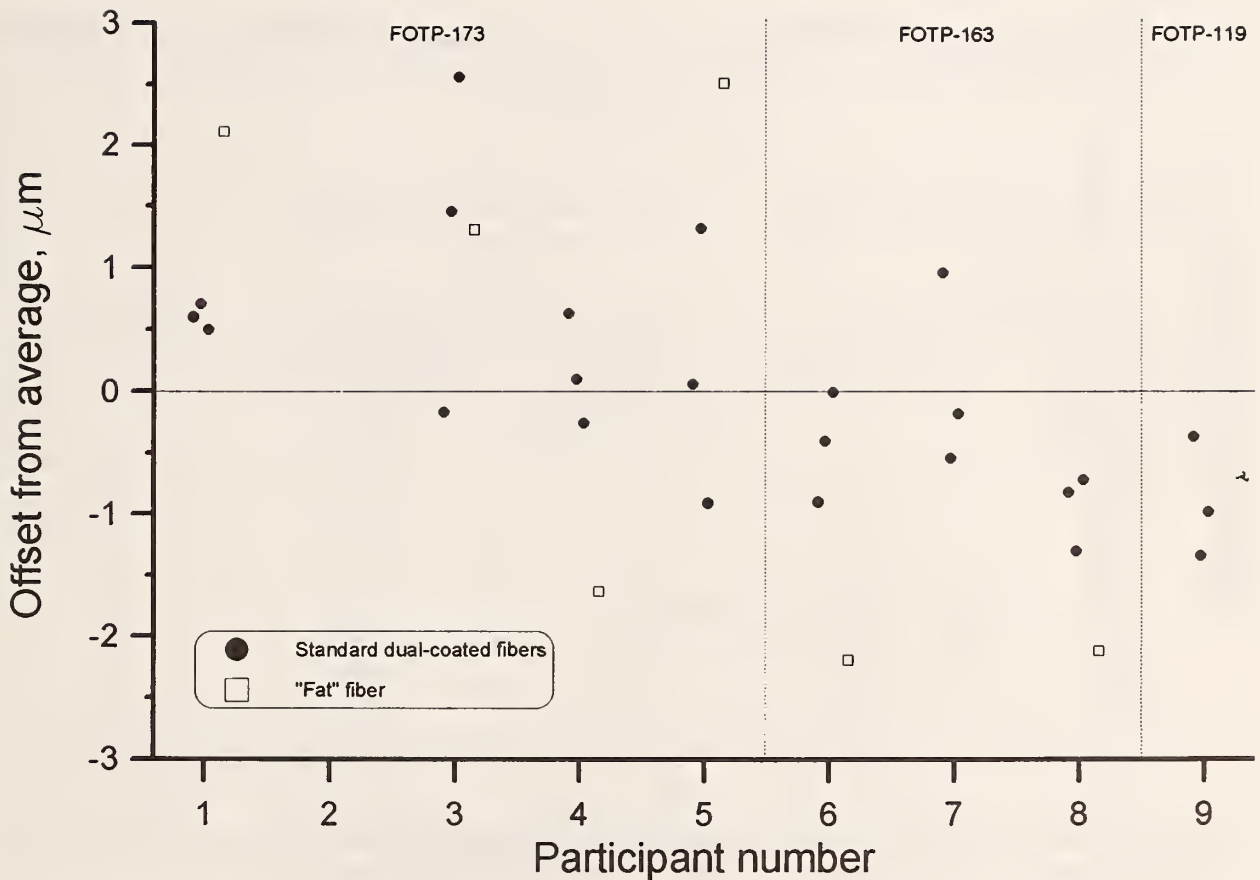
Figure 12. Offsets of participants' fiber coating outer layer maximum wall thickness measurements from average values. Up to six points plotted, for each participant, represent the six fibers in the measurement sample. Filled symbols denote standard 250 μm dual-coated fibers. Open symbols denote non-standard fibers: single-coated, hermetically coated, and "fat" (nominally 500 μm). Participants are grouped according to their measurement methods, identified by TIA Fiber Optic Test Procedure (FOTP) numbers.
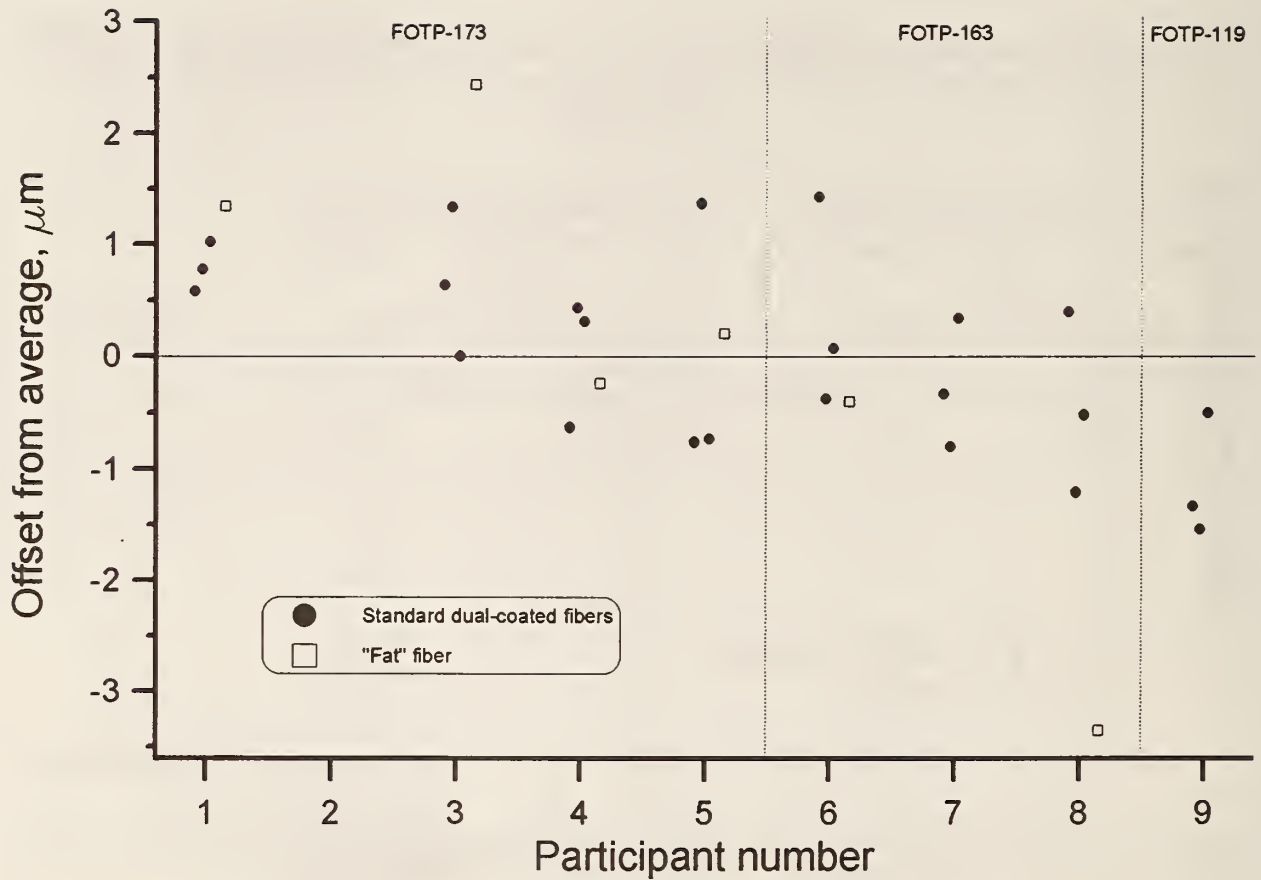
Table 8. Statistics for participants' outer layer fiber coating minimum and maximum wall thickness measurement offsets from average values, including only standard 250 µm dual-coated fibers.

Participant	Outer layer minimum wall thickness offsets from average values (standard dual-coated fibers)		Outer layer maximum wall thickness offsets from average values (standard dual-coated fibers)	
	Average offset, µm	Standard deviation of offsets, µm	Average offset, µm	Standard deviation of offsets, µm
1	−1.80	0.76	−1.54	0.58
3	+1.02	1.24	+0.23	0.41
4	+0.84	0.51	+1.73	0.70
5	−2.22	1.30	−2.98	1.82
6	+1.42	0.13	+1.40	0.23
7	−1.10	0.74	−0.31	0.61
8	+1.25	0.30	+1.06	0.54
9	+0.59	1.44	+0.40	1.97
	Average offset magnitude,[a] µm	Average offset spread,[b] µm	Average offset magnitude,[a] µm	Average offset spread,[b] µm
	1.28	**0.80**	**1.21**	**0.86**

[a]Average of absolute values of participants' average offsets.

[b]Average of participants' offset standard deviations.

Figure 13. Offsets of participants' fiber coating inner layer minimum wall thickness measurements from average values. Up to four points plotted, for each participant, represent those of the six fibers in the measurement sample for which measurements of this parameter were made. Filled symbols denote standard 250 μm dual-coated fibers. Open symbols denote a non-standard, "fat" (nominally 500 μm) fiber. Participants are grouped according to their measurement methods, identified by TIA Fiber Optic Test Procedure (FOTP) numbers.

Figure 14. Offsets of participants' fiber coating inner layer maximum wall thickness measurements from average values. Up to four points plotted, for each participant, represent those of the six fibers in the measurement sample for which measurements of this parameter were made. Filled symbols denote standard 250 μm dual-coated fibers. Open symbols denote a non-standard, "fat" (nominally 500 μm) fiber. Participants are grouped according to their measurement methods, identified by TIA Fiber Optic Test Procedure (FOTP) numbers.

Table 9. Statistics for participants' inner layer fiber coating minimum and maximum wall thickness measurement offsets from average values, including only standard 250 μm dual-coated fibers.

Participant	Inner layer minimum wall thickness offsets from average values (standard dual-coated fibers)		Inner layer maximum wall thickness offsets from average values (standard dual-coated fibers)	
	Average offset, μm	Standard deviation of offsets, μm	Average offset, μm	Standard deviation of offsets, μm
1	+0.60	0.11	+0.79	0.22
3	+1.28	1.37	+0.66	0.67
4	+0.16	0.45	+0.04	0.58
5	+0.16	1.12	−0.04	1.22
6	−0.44	0.44	+0.38	0.94
7	+0.08	0.79	−0.26	0.57
8	−0.94	0.31	−0.44	0.81
9	−0.90	0.49	−1.12	0.55
	Average offset magnitude,[a] μm	**Average offset spread,[b] μm**	**Average offset magnitude,[a] μm**	**Average offset spread,[b] μm**
	0.57	**0.64**	**0.47**	**0.70**

[a]Average of absolute values of participants' average offsets.

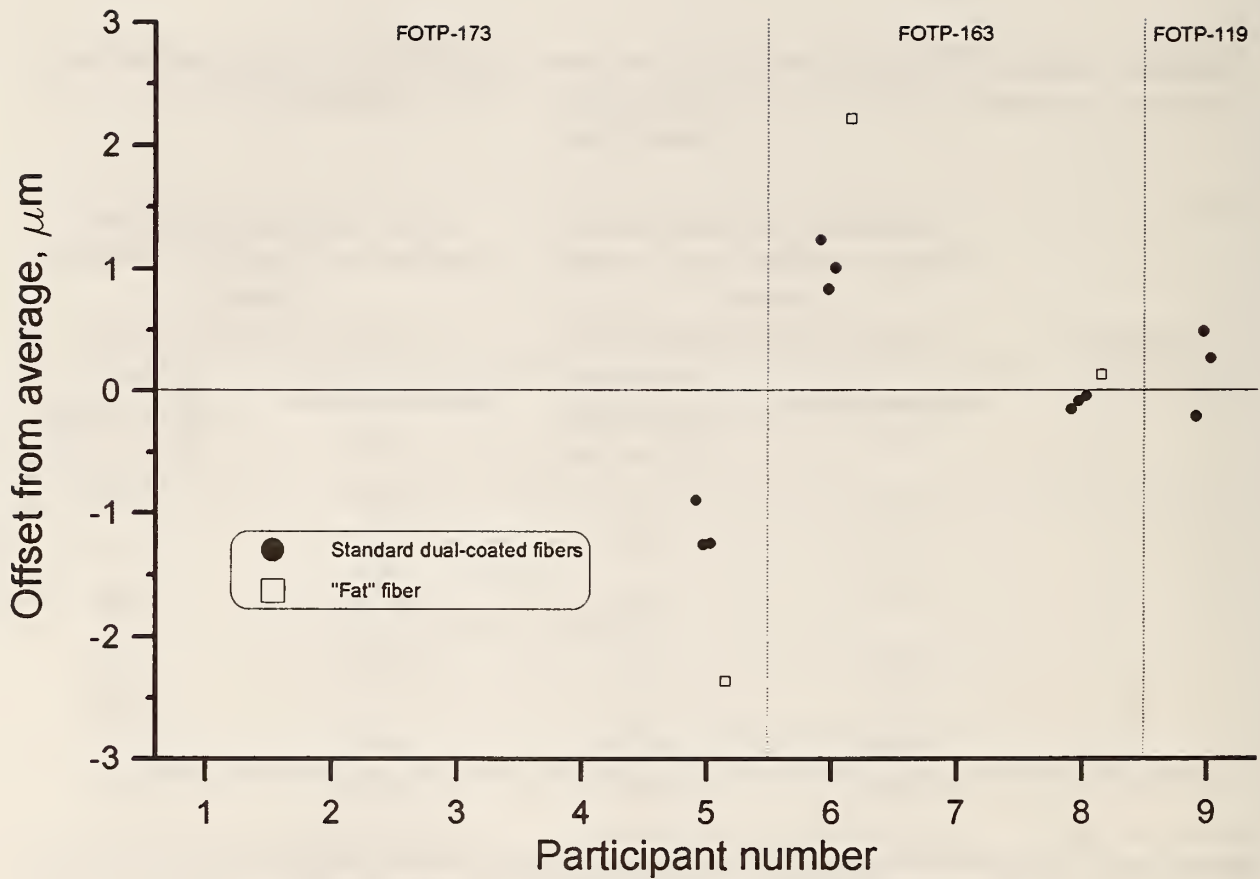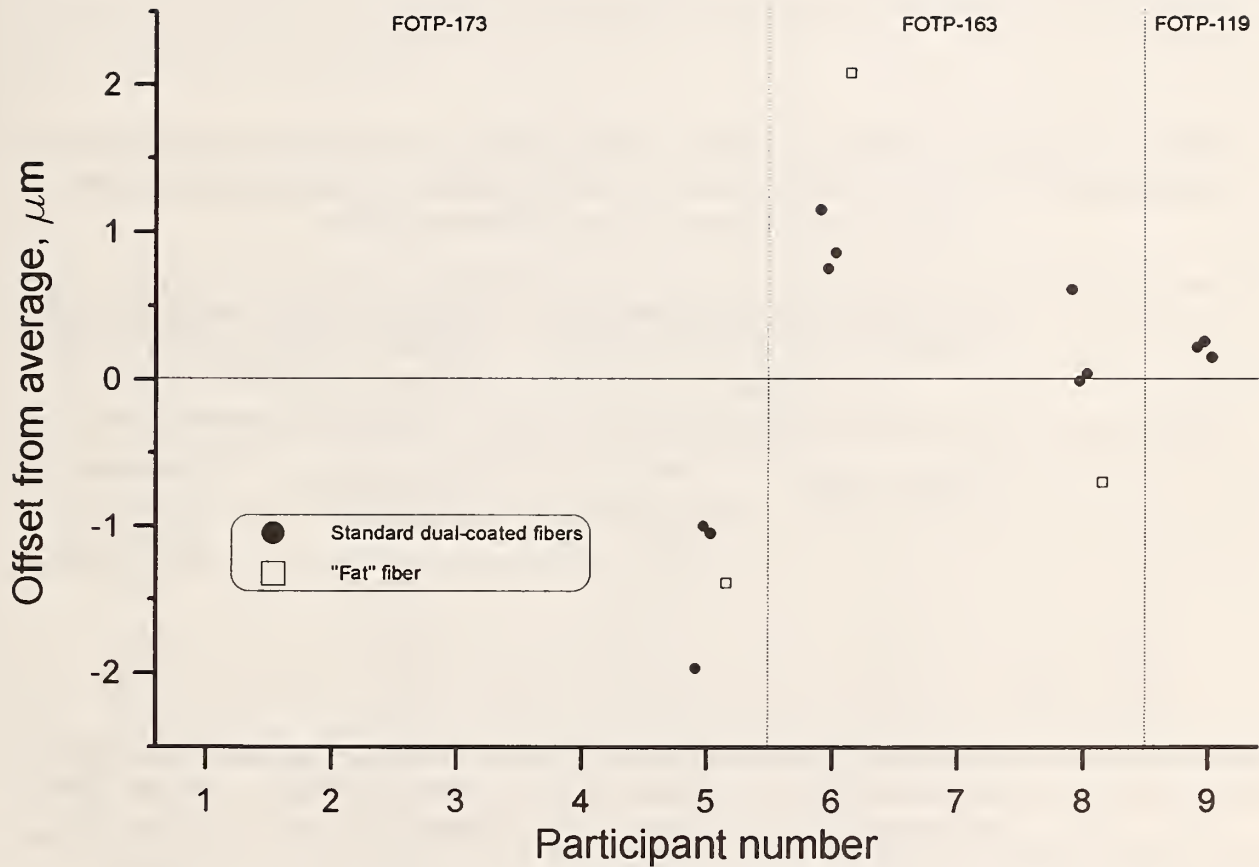[b]Average of participants' offset standard deviations.

Figure 15. Offsets of participants' fiber coating combined (outer and inner layers) minimum wall thickness measurements from average values. Up to four points plotted, for each participant, represent those of the six fibers in the measurement sample for which measurements of this parameter were made. Filled symbols denote standard 250 μm dual-coated fibers. Open symbols denote a non-standard, "fat" (nominally 500 μm) fiber. Participants are grouped according to their measurement methods, identified by TIA Fiber Optic Test Procedure (FOTP) numbers.

Figure 16. Offsets of participants' fiber coating combined (outer and inner layers) maximum wall thickness measurements from average values. Up to four points plotted, for each participant, represent those of the six fibers in the measurement sample for which measurements of this parameter were made. Filled symbols denote standard 250 μm dual-coated fibers. Open symbols denote a non-standard, "fat" (nominally 500 μm) fiber. Participants are grouped according to their measurement methods, identified by TIA Fiber Optic Test Procedure (FOTP) numbers.

35

Table 10. Statistics for participants' fiber coating minimum and maximum wall thickness measurement offsets from average values, for combined (inner and outer) coating layers, including only standard 250 μm dual-coated fibers.

Participant	Combined layers minimum wall thickness offsets from average values (standard dual-coated fibers)		Combined layers maximum wall thickness offsets from average values (standard dual-coated fibers)	
	Average offset, μm	Standard deviation of offsets, μm	Average offset, μm	Standard deviation of offsets, μm
5	−1.12	0.21	−1.34	0.54
6	+1.03	0.20	+0.92	0.20
8	−0.09	0.05	+0.21	0.34
9	+0.19	0.36	+0.21	0.06
	Average offset magnitude,[a] **μm**	**Average offset spread,**[b] **μm**	**Average offset magnitude,**[a] **μm**	**Average offset spread,**[b] **μm**
	0.61	**0.21**	**0.67**	**0.29**

[a]Average of absolute values of participants' average offsets.

[b]Average of participants' offset standard deviations.

4. Connector Ferrule Comparisons

Ceramic ferrules are widely used as components in most optical fiber connectors. Tolerances on outside diameter, concentricity, and roundness (and to a lesser extent, surface roughness, straightness, and exit angle) of ferrules determine how well and repeatably connectors can be mated. Tolerance on the inside (bore) diameter of the ferrules is also important, determining how snug the fit of the fiber will be and, hence, how well the fibers will be aligned in a connection.

4.1 Ferrule Inside (Bore) Diameter

NIST, at the request of the TIA, coordinated an interlaboratory comparison of measurements of ferrule inside diameter (ID) among mostly North American TIA members. 36 ceramic ferrules were measured. A numbered tab was attached to each ferrule to preserve identity. According to specified nominal ID values supplied by the manufacturer, the set of ferrules included one each of 123 μm and 127 μm ID, four each of 124 μm and 126 μm ID, and twenty-six 125 μm ID ferrules. These ferrules were numbered randomly for measurement by participants.

There were two general types of measurement method. The first was a series of go/no-go measurements, using a calibrated set of pin gages [14] or fibers. The nominal diameters of these pin gages were typically integral numbers of micrometers. In the typical implementation, a user attempts to push the various pin gages, in increasing order of diameter, through the bore in the ferrule. The largest pin gage to pass through the ferrule (a "go" measurement) determines essentially the lower bound of the ferrule ID; it is an underestimate of up to 1 μm (or whatever increment of diameter is used) of the true ID. The second type of measurement used in this comparison was video, in which the ferrule IDs were measured by video analysis of the ferrule endfaces. Due to the substantial differences between the two types of methods, particularly resolution differences, we will present the go/no-go and video results separately.

There were ten participants who used the go/no-go method, and they were assigned numbers, 1 through 10, in roughly chronological order of participation. Nine used pin gages; one used fibers. Participants measured each ferrule twice, going through them in numerical order first, then in reverse numerical order. Any bias due to degradation of the pin gages or fibers from repeated insertions should have shown up in this measurement scheme. Results

are shown in figure 17, a plot of disagreements from specified nominal ID versus ferrule (arranged according to nominal ID). Each plotted point represents one participant who disagreed with the specified nominal ID for that ferrule and shows by how much that participant disagreed. A diamond denotes repeated disagreements on both measurements of the ferrule, while a triangle denotes a nonrepeated (one-time) disagreement. There were three cases of ±2 μm disagreement, all on the 123 μm and 127 μm ferrules. There are more ±1 μm disagreements, although 27 of the repeated (diamond) −1 μm points are from one participant (number 6).

Table 11 shows the number of disagreements per participant and expresses a disagreement rate as a percentage of the total number of measurements. Overall numbers, as well as numbers for each nominal ID, are also given. These numbers are shown with and without the data of Participant 6 included. Participant 10 used fibers rather than pin gages but has a disagreement rate in line with the average. Participant 7 used 0.5 μm steps in pin gage diameter but shows a higher than average disagreement rate. Participants 8 and 9 also used twice the normal number of pin gages, with gages just larger and just smaller than each nominal (integral) diameter, and both show significantly lower disagreement rates than average; in fact, Participant 9 has a disagreement rate of 0, agreeing with specified nominal ferrule ID on every measurement made. The overall disagreement rate of 14.2 percent, which is high enough to be of concern, reduces to 7.4 percent if we disregard Participant 6. If we look at measurements on only nominally 125 μm ID ferrules, which composed the largest sample in the comparison and are one of the most widely used diameters, and if we again disregard Participant 6, we see a disagreement rate of 2.6 percent. This rate, if typical for the industry, seems very good, given the resolution of the measurement technique.

One unexplained result is that disagreement rate was not uniform for different nominal IDs. While sample sizes were smaller for nominal IDs other than 125 μm, we can compare disagreement rates between nominal IDs that had equal sample size; with or without Participant 6, the disagreement rate for 124 μm ferrules was significantly larger than for 126 μm, and the disagreement rate for the one 123 μm ID ferrule was significantly larger than for the one 127 μm ferrule.

Three participants used video methods to measure ferrule ID. Video Method 1 used a reflected light (front-lighted) system. They fitted an ellipse to their ferrule bore edge data and reported the diameter of the minor axis, to correspond to the largest-diameter fiber that could fit in the ferrule bore. Video Methods 2 and 3 used back-lighted systems and reported average diameter or diameter of a fitted circle. All video measurements were made after the

go/no-go measurements had been completed, so some of the ferrule endfaces and bore edges were in poor condition (chipped and/or dirty). Each video participant reported their observations on the condition of each of the ferrules.

Figure 18 shows the results of the video measurements as a plot of disagreement of measurements from specified nominal ferrule ID versus ferrule (arranged according to nominal ID). Filled symbols denote ferrules that were reported, by a given participant, to be in fair or good condition; open symbols denote ferrules reported to be in poor condition. Lines connect data, for a given participant, for ferrules that were reported by *all* participants to be in fair or good condition. Each video method shows systematic disagreement with nominal values and considerable random spread. The lines show little correlation among any of the three data sets. The sign of the disagreement does not seem to be related to front-lighted versus back-lighted systems, since Video Methods 1 (front-lighted) and 3 (back-lighted) have the same sign.

We calculated the average offset from the specified nominal ferrule IDs and the standard deviation of the offsets about this average, for each video method. These results are shown in table 12, both with all ferrules included and disregarding those in poor condition. The video methods do not appear to be preferable alternatives to the go/no-go method. If the standard deviations were small, then the average offsets could be minimized by calibration. Also, the standard deviation for any one video method *could* be a real tracking of differences of true ferrule IDs from specified nominal values, but this does not seem likely, given the relatively good and consistent agreement with the nominal values in the go/no-go measurements. A factor limiting the usefulness of the video methods is that the diameter is measured at the ferrule endface; potential tapering in the bore along the length of the ferrule is not detected.

In conclusion, the go/no-go method, in spite of its limitations, seems to give dependable results for ferrule ID measurements, especially for typical (125 μm) ferrule IDs. Improving resolution by including sub-micrometer steps in pin gage diameter may increase accuracy and certainly increases confidence. Since the only published test procedure is for the go/no-go method using 1 μm steps in pin gage diameter, tolerances on ferrule IDs are pretty much limited to the resolution (typically a 1 μm range) of the measurement method.
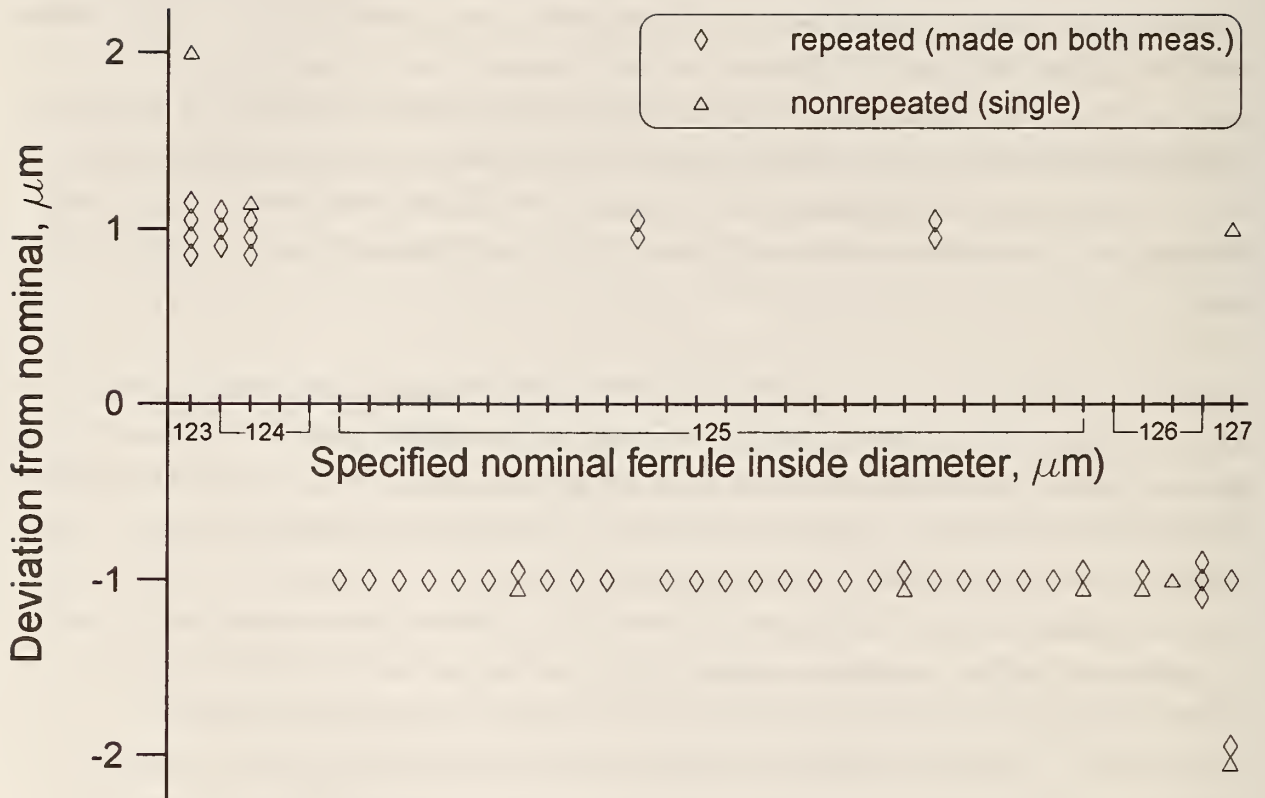
Figure 17. Results for ferrule inside (bore) diameter measurements using go/no-go method. Each plotted point represents one participant who disagreed with the specified nominal value for a given ferrule. The y-axis shows the disagreement. Only disagreements are shown. Each participant measured each ferrule twice. Diamonds denote repeated disagreement (same for both measurements), while triangles denote nonrepeated (one-time) disagreements. Twenty-seven of the points at −1 μm are from one participant.

Table 11. Results for ferrule inside (bore) diameter (ID) measurements using go/no-go method, compared to specified nominal values. Participants used pin gages with diameters that were nominally integral numbers of micrometers, except as noted. Participant 6 (shaded) disagreed with nominal values considerably more than other participants, so overall numbers are calculated with and without Participant 6.

Participant	Total number of measurements	Total number of disagreements with specified nominal IDs	Disagreement rate, %
1	72	5	6.9
2	72	2	2.8
3	72	4	5.6
4	72	10	13.9
5	72	8	11.1
6	72	54	75.0
7[a]	72	10	13.9
8[b]	72	2	2.8
9[b]	72	0	0.0
10[c]	72	7	9.7
Overall all participants	720	102	**14.2**
Overall without Participant 6	648	48	**7.4**

Specified Nominal ID, μm	Including all participants			Disregarding Participant 6		
	Total number of measurements	Total number of disagreements	Disagreement rate, %	Total number of measurements	Total number of disagreements	Disagreement rate, %
123	20	9	**45.0**	18	9	**50.0**
124	80	15	**18.8**	72	15	**20.8**
125	520	62	**11.9**	468	12	**2.6**
126	80	10	**12.5**	72	8	**11.1**
127	20	6	**30.0**	18	4	**22.2**

[a]Used 0.5 μm steps in pin gage size.

[b]Used pin gages just smaller *and* just larger than integral numbers of micrometers.

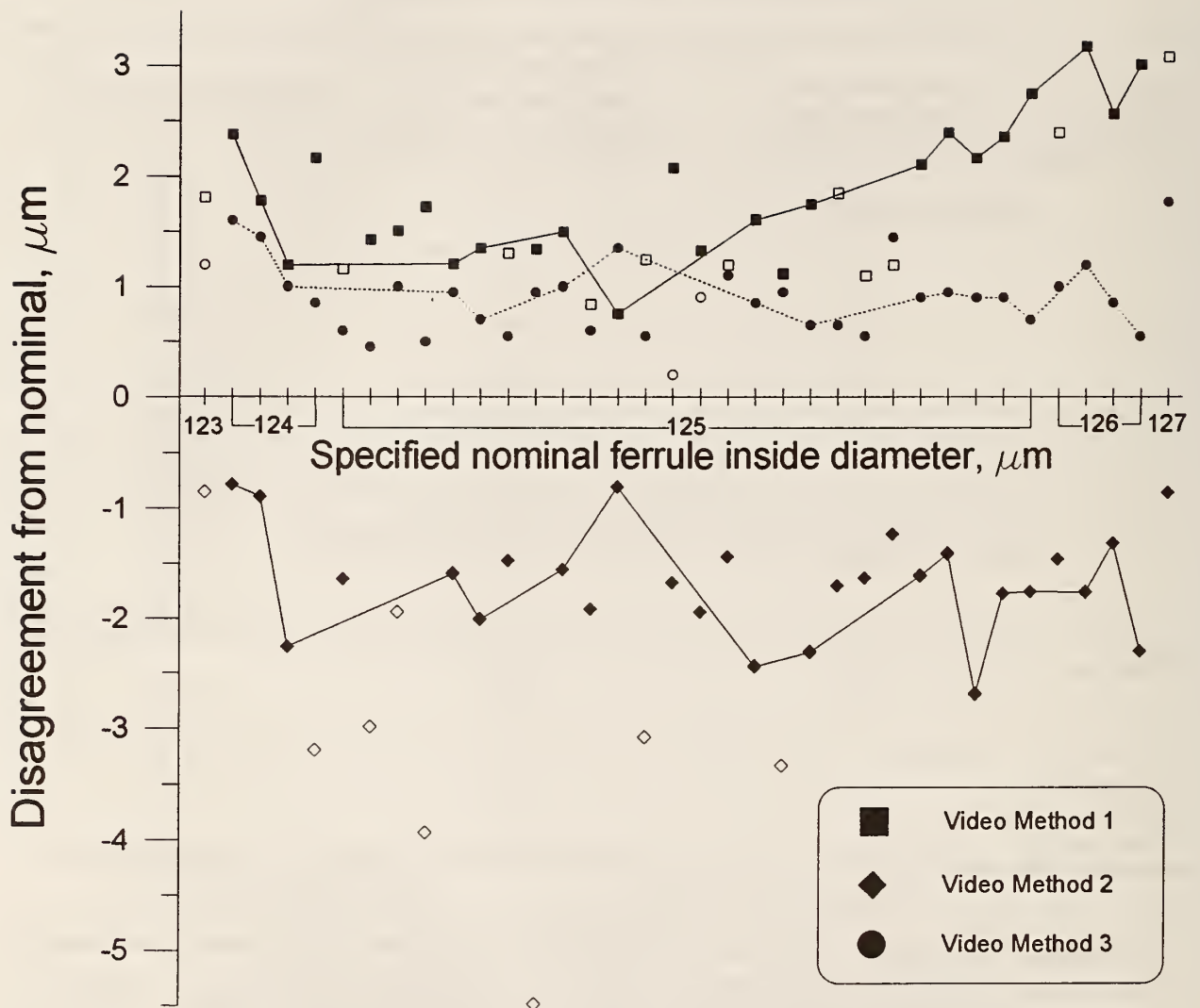[c]Used fibers rather than pin gages.

Figure 18. Results for ferrule inside (bore) diameter measurements using video methods. Open symbols denote ferrules that were seen by a given method as being in poor (dirty, chipped, etc.) condition. Lines connect data, for a given participant, for ferrules that were reported by *all* participants to be in fair or good (undamaged, clean, etc.) condition.

Table 12. Statistics for ferrule inside (bore) diameter (ID) measurements using video methods. Averages and standard deviations of participants' offsets from specified nominal values are shown, for measurements on all ferrules, and disregarding ferrules, for each given participant, that were reported to be in poor condition.

Participant	Average offset from specified nominal IDs, µm	Standard deviation of offsets, µm
Video method 1	+1.78	0.65
Video method 2	−1.97	0.96
Video method 3	+0.90	0.34
Disregarding data from "poor" (chipped, dirty, etc.) ferrules		
Video method 1	+1.87	0.63
Video method 2	−1.65	0.49
Video method 3	+0.91	0.33

4.2 Pin Gage Diameter

As part of the ferrule ID comparison, NIST invited go/no-go participants to provide us with the pin gages used in their measurements; subsequently, the diameters of the pin gages were measured with the NIST contact micrometer. In this small measurement sample, several pin gages appeared to be outside of specified tolerances. This could have been due to problems with manufacturers' specified tolerances or to degradation of the pin gages from repeated insertions into the harder ceramic ferrules. The TIA test procedure for ferrule ID measurements [14] requires the use of pin gages with diameters traceable to NIST and tolerances of +0.25/−0.00 μm (that is, diameters equal to the nominal value or no more than 0.25 μm greater). Accuracy of pin gage manufacturers in meeting specified tolerances is beyond the scope of discussion here. However, traceability to NIST should be improved with the availability of a NIST pin gage diameter SRM, which will be available from the NIST SRM Program in late 1995 or early 1996 [15]. Possible degradation of the pin gages with repeated use means that users need to periodically verify that diameters are still within specifications.

The TIA requested that NIST coordinate an interlaboratory comparison, to check the precision and accuracy of such measurements. The measurement sample consisted of 18 pin gages, 6 each, of nominally 125 μm, 126 μm, and 127 μm diameter. Diameter was measured at the midpoint along the length of each pin gage. Each reported value was the average of at least three measurements. Besides our contact micrometer measurements, there were seven participants. One participant (number 2) was our colleagues in the Precision Engineering Division of NIST (in Gaithersburg, MD). The others were various commercial laboratories. One participant used a laser micrometer; all others used contact methods. Among the contact methods, some determined relative position interferometrically while others did so mechanically. There were no obvious method-dependent biases. All NIST measurements were corrected for compression, which occurs at the contact points between the measurement specimen and the jaws of the micrometer; a compression-corrected contacting measurement should yield the same value as an accurate noncontact method.

Table 13 shows measurement spreads per pin gage for all reported measurements. The average value was 0.3 μm. Sixteen of eighteen pin gages had spreads between 0.21 μm and 0.39 μm. One had a significantly larger spread of 0.43 μm, and one was significantly smaller at 0.14 μm. These two could have been statistical anomalies, or they may have been significantly different in diameter uniformity than what was typical for pin gages in this measurement sample.

Figure 19 plots participant data offsets from the NIST-Boulder contact micrometer. 18 points per participant represent the 18 pin gages measured. Agreement between the two NIST locations is verified here. The offsets of the other participants' data show definite systematic components. Some also have large random components. For each participant, the 18 plotted points represent, from left to right, the nominally 125 μm pin gages, then 126 μm, and finally 127 μm. Some participants seem to show a slightly different systematic offset for each of the three nominal sizes. This is especially apparent for Participant 4 and to a lesser extent, for Participants 5, 6, and 7. This points to a possible need for separate calibrations for each of the nominal diameters.

An average offset and the standard deviation (or offset spread) of the eighteen offsets about that average can be calculated for each participant. These statistics are shown in table 14. The average offset magnitude of 0.217 μm is nearly twice as large as the average offset spread of 0.113 μm, so a typical participant could improve their overall accuracy considerably by use of a calibration artifact such as a NIST SRM. The offset magnitude would reduce with such a calibration, and even the offset spread may reduce, if a separate calibration is done for each nominal diameter of pin gage.

Roughly speaking, the offset magnitudes give an indication of the accuracy of participants' measurements, while the offset spreads give an indication of precision. Currently, the typical participant does not have the accuracy to verify whether pin gages are within diameter specifications. The precision of most participants, however, appears to be good enough to allow such verifications, if test sets are properly calibrated.

Table 13. Measurement spreads (1 standard deviation) for each pin gage, for diameter measurements. Measurements were made at the mid-point along the length of each pin gage.

Pin gage specimen number	Mid-point diameter measurement spread (1 standard deviation), µm
1	0.26
2	0.31
3	0.28
4	0.35
5	0.29
6	0.33
7	0.28
8	0.26
9	0.21
10	0.31
11	0.43
12	0.31
13	0.39
14	0.25
15	0.14
16	0.35
17	0.32
18	0.27
Average	0.30
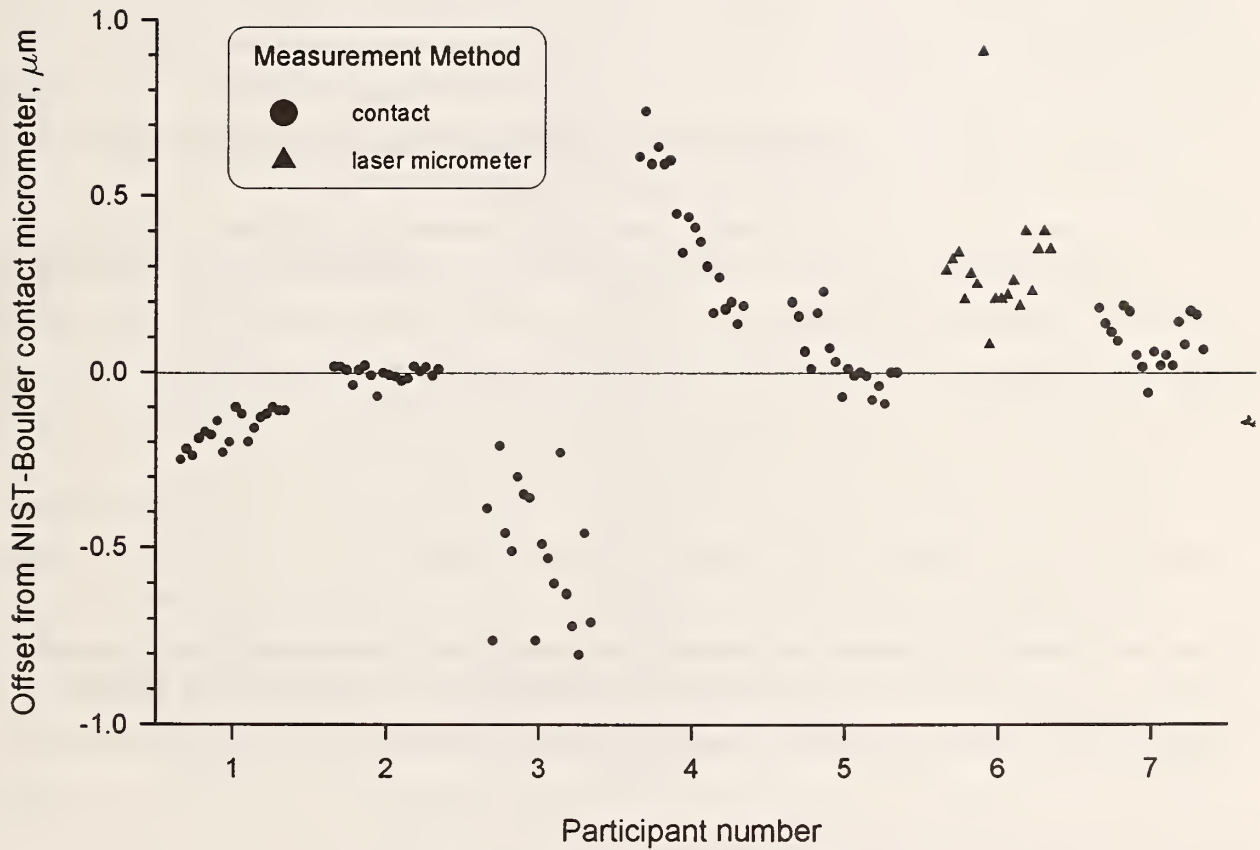
Figure 19. Offsets of participants' pin gage diameter measurements from NIST-Boulder contact micrometer. Eighteen points plotted for each participant represent the eighteen pin gages in the measurement sample. Participant 2 represents other NIST data, from the Precision Engineering Division in Gaithersburg, MD.

Table 14. Statistics for participants' pin gage diameter measurement offsets from NIST-Boulder contact micrometer.

Participant	Average offset, μm	Standard deviation of offsets, μm
1	−0.165	0.051
2[a]	−0.004	0.023
3	−0.515	0.187
4	+0.402	0.191
5	+0.036	0.096
6	+0.306	0.171
7	+0.093	0.072
	Average offset magnitude,[b] μm	**Average offset spread,[c] μm**
	0.217	**0.113**

[a]NIST-Gaithersburg (Precision Engineering Division).

[b]Average of absolute values of participants' average offsets.

[c]Average of participants' offset standard deviations.

4.3 Ferrule Geometry

This TIA/NIST interlaboratory comparison dealt with measurements of ferrule outside diameter (OD) and ferrule concentricity (more properly, bore/ferrule concentricity error) on 20 ferrules, as well as measurements, on a subset of 3 of the ferrules, of roundness (actually noncircularity, defined as maximum radius minus minimum radius) and surface finish, defined as average roughness (R_A: the arithmetic-average deviation from a smooth surface, over a user-defined scan length). Measurements of ferrule straightness and exit angle (an indicator of bore straightness) were also solicited on the subset of three ferrules, but not enough participants made these measurements to include any analyses or results here (two made some exit angle measurements; none made straightness measurements).

There were eight participants from industry, as well as OD and roundness measurements from the Precision Engineering Division of NIST-Gaithersburg. NIST is working on an SRM for ferrule OD, which will be available in late 1995 or early 1996 [16]. The NIST ferrule OD measurements were considered reference values and therefore the values to which participants' ferrule OD measurements were compared. NIST measurements were corrected for compression, which occurs at the contact points between the measurement specimen and the jaws of the micrometer. Ferrule OD is the only one of the measured parameters to have a required tolerance in TIA documents [17]; a range between 2.4985 mm and 2.4995 mm is specified, implying a nominal value of 2.499 mm and a tolerance of ±0.5 μm. To confidently meet this tolerance, agreement between participants and measurement accuracy on the order of about ±0.05 μm is desirable. One participant withdrew from the comparison, so results from seven participants, numbered 1 through 7, are reported here.

The measurement specimens were provided by one manufacturer, from regular production runs, to represent typical, off-the-shelf ferrules. Specimens were identified by randomly assigned numbers, 1 through 20. The ferrules could not be permanently marked directly, and for these measurements, we could not attach any sort of identifying tabs, so ferrules were placed in individually numbered, resealable bags, and participants were instructed to open only one bag at a time, to preserve identification throughout the comparison.

For ferrule OD measurements, three participants used laser micrometers, while four participants plus NIST used mechanical contact methods. There is currently no TIA test procedure for ferrule OD. Measurements were made at the midpoint of the length of each

ferrule. For concentricity measurements, four participants used mechanical methods, in which, typically, a pin gage is inserted into the ferrule hole, and the stylus of a profilometer measures the deflection of the hole/gage as the ferrule is rotated. One participant used a proprietary method. Two participants used optical methods, in which deflection of a video image of the ferrule hole is measured as the ferrule is rotated. There is a draft TIA document [18] for ferrule concentricity.

For OD and concentricity, participants were instructed to measure the ferrules in numerical order and then repeat the measurements in reverse numerical order. Such a scheme was intended to identify any wearing or degradation of the ferrules or the V-grooves (or other test set fixturing) used to hold the ferrules during measurements. No bias between numerical and reverse data was observed in any participant's data, so averages of the two reported measurements on each ferrule were used in results presented here.

Roundness and surface finish measurements were made only on ferrules 5, 10, and 15, by those participants who had the capabilities. Only mechanical methods, using profilometers, were used. All instruments were commercial products, from four different manufacturers, and many were made specifically for either roundness or surface finish measurements. There was no apparent systematic bias between instruments from different manufacturers. Roundness measurements were made approximately 1 mm from the exit (polished) ends of the ferrules. Four participants, as well as NIST, made these measurements. Four participants measured surface finish; they were instructed to make the measurements *near* the exit ends of the ferrules and also to report their scan length. There are currently no TIA test procedures for roundness or surface finish measurements.

Table 15 shows the measurement spreads (1 standard deviation) for each ferrule, for each parameter measured, as well as average values. The average spread of 0.35 μm for ferrule OD is not small enough to meet desired tolerances. This is shown in figure 20, a plot of offsets of ferrule OD measurements from NIST contact micrometer measurements versus participant number. 20 points plotted for each participant represent the 20 ferrules measured. Three ferrules (1, 14, and 15) regularly gave substantially low or high offsets compared to typical values for given participants, perhaps due to dirtiness, imperfections, or nonuniformities on the ferrules. These ferrules are identified by open symbols. Filled circles represent laser micrometer data; filled squares represent mechanical measurements. The data from the two types of methods bracket each other well, so there are no obvious systematic differences between methods. Even if we disregard data from the three extreme ferrules, many data points lie outside the desired ±0.5 μm tolerance. There are however, obvious

systematic components to the participants' offsets, as evidenced by the clumping of each participant's offset data. Calibration by an artifact such as a NIST SRM can be expected to improve the agreement significantly.

Figure 21 is the same type of plot for ferrule concentricity, except that offsets from average measured values are shown. Again, there were three ferrules (1, 14, and 17 in this case) that regularly gave substantially low or high offsets, relative to participants' typical offsets. These three are denoted by open symbols. Filled circles show data from mechanical methods. Filled squares represent data from optical methods. Filled diamonds represent data from the one proprietary method. Except for Participant 4, there are not large systematic components to the overall spreads; rather the spreads appear to be mostly random. This means that interlaboratory agreement of concentricity measurements is limited mostly by the precision of the measurement test sets. This further indicates that a calibration artifact for ferrule concentricity would not be of much value. There appears to be a possible small systematic difference between methods. Most optical measurements were slightly less than corresponding mechanical measurements. However, there were only two optical data sets (Participants 6 and 7), and one mechanical data set (Participant 4) similarly had relatively low measured values. Also, the participant order is roughly chronological, so both sets of optical measurements were made near the end of the comparison, and it is possible that their relatively low measured values were due to degradation of the ferrule specimens. On the other hand, NIST measurements were also made near the end of the comparison (between Participants 6 and 7), and we do not see better agreement with the NIST measurements for optical methods than for mechanical methods.

For these ferrule OD and concentricity measurements, we calculated the average of each participant's 20 offset values and the standard deviation (or offset spread) of those offsets about that average. These statistics are shown in table 16. As visually shown in figure 20, the average ferrule OD offset magnitude is considerably greater than the average offset spread, so overall agreement should be improved by calibration. Conversely, as shown in figure 21, the average concentricity offset magnitude is considerably smaller than the average offset spread, so calibration would not be expected to improve agreement. For ferrule OD, though, even accurate calibration of all participants' test sets would not reduce the measurement spread any lower than on the order of the average offset spread of 0.19 μm (1 standard deviation), which is limited by the precision of the participants' measurements. Such a measurement spread, if realized, would be an improvement, but it is probably not low enough to support the industry tolerance of ±0.5 μm.

Results for roundness are shown in figure 22 and for surface finish in figure 23. Each measured value is plotted on these graphs, and the dotted lines connect the averages for each ferrule. Measurements by a subset of participants on a few ferrules did not yield enough information to do in-depth statistical analyses for these parameters, but we can make some general comments. The measurement spreads for ferrule roundness were high, given the resolution of the profilometers. We initially thought that participants might have used different roundness definitions, but a review of what was reported, as well as some follow-up discussions, verified that all used the same definition. However, probe diameters on the instruments varied significantly; participants reported probe diameters ranging from 0.2 mm to 2 mm. Such a difference in probes may well account for the observed measurement spreads, although there was no definite systematic correlation between probe diameter and roundness measurements. Also, NIST measurements were systematically low. This may be because NIST values were calculated based on 12 points taken around the circumference of the ferrules, while all other participants used much finer sampling (number of sampling points greater by an order of magnitude or more). The spreads for surface finish measurements were somewhat less than for roundness but still somewhat high for the instruments used. Again probe diameter was possibly a factor. Additionally, participants measured over different scan lengths, ranging from 2.5 mm to 4 mm, which could have affected the spreads.

In conclusion, while OD is the only one of the ferrule parameters to currently have an agreed-upon tolerance, measurements in this comparison suggest that the industry may have trouble meeting the desired tolerance of ±0.5 μm, given typical measurement precision, even with accurate calibration. A calibration artifact such as a NIST SRM will nevertheless improve interlaboratory agreement. Probe diameter and scan length are important parameters that should be specified for profilometer measurements of quantities such as ferrule roundness and surface finish.

Table 15. Measurement spreads (1 standard deviation) for all measurements made on each ferrule, for all parameters measured.

Ferrule	Outside diameter, μm	Concentricity, μm	Roundness $(r_{max} - r_{min})$, μm	Surface finish (R_A), μm
1	0.8	0.55		
2	0.3	0.16		
3	0.4	0.40		
4	0.3	0.34		
5	0.3	0.22	0.102	0.015
6	0.3	0.23		
7	0.4	0.20		
8	0.3	0.16		
9	0.4	0.15		
10	0.3	0.29	0.061	0.013
11	0.3	0.09		
12	0.3	0.25		
13	0.3	0.19		
14	0.2	0.19		
15	0.5	0.23	0.056	0.021
16	0.3	0.19		
17	0.3	0.62		
18	0.3	0.10		
19	0.3	0.17		
20	0.4	0.21		
Average	**0.35**	**0.25**	**0.073**	**0.016**
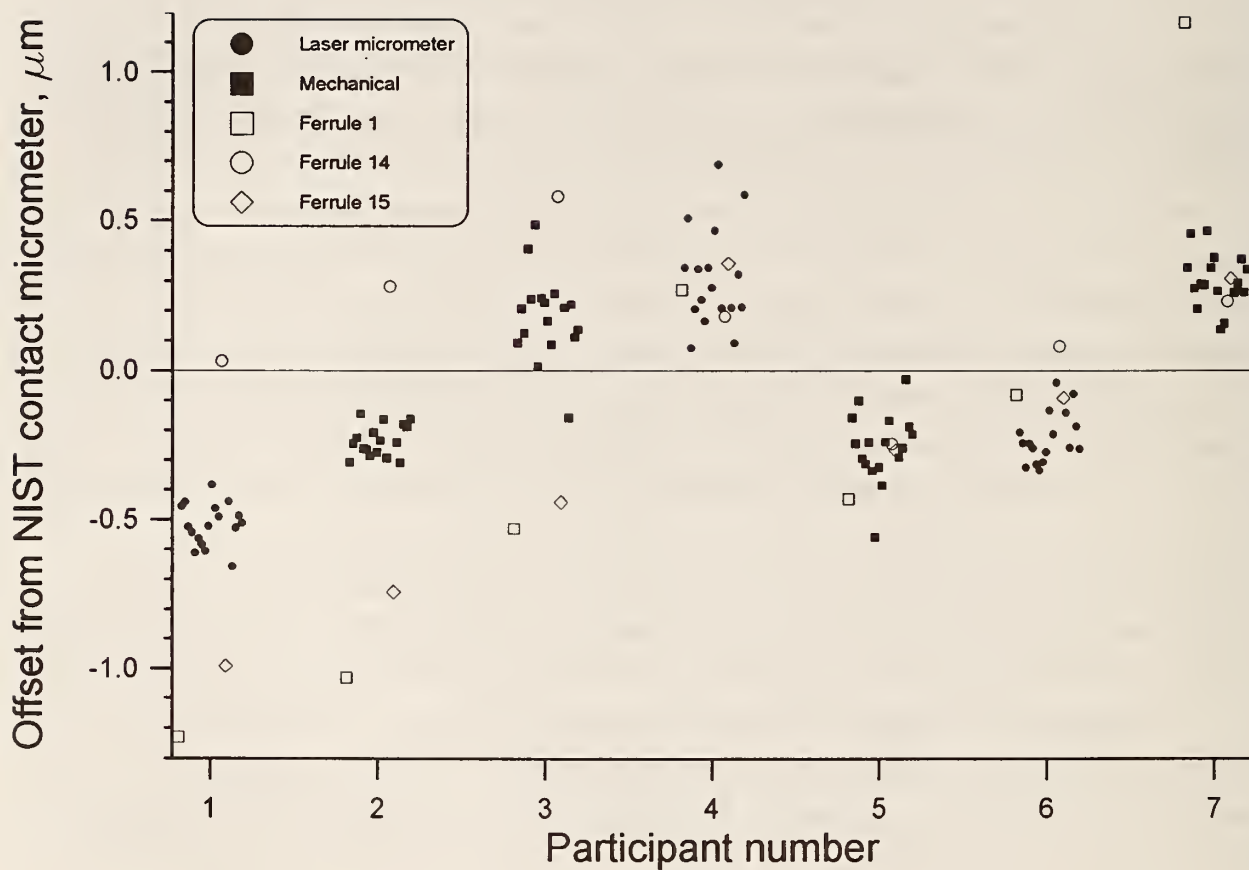
Figure 20. Offsets of participants' ferrule outside diameter measurements from NIST contact micrometer. Twenty points plotted, for each participant, represent the twenty ferrules in the measurement sample. Open symbols denote three ferrules that regularly gave substantially low or high offset values compared to typical values for given participants. Filled circles represent measurements by laser micrometers. Filled squares represent measurements by mechanical methods.
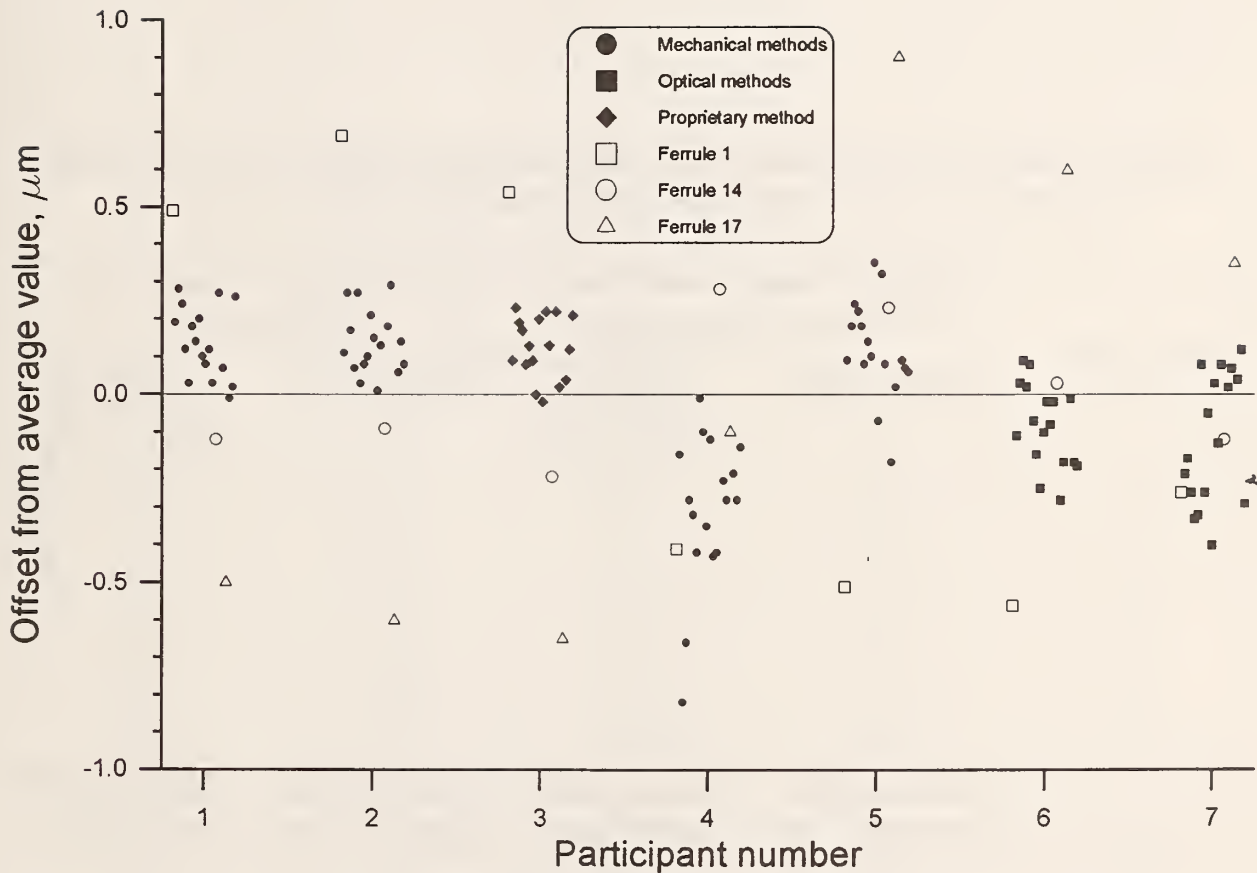
Figure 21. Offsets of participants' ferrule concentricity measurements from average values. Twenty points plotted, for each participant, represent the twenty ferrules in the measurement sample. Open symbols denote three ferrules that regularly gave substantially low or high offset values compared to typical values for given participants. Filled circles represent measurements by mechanical methods. Filled squares represent measurements by optical methods. Filled diamonds represent measurements from one participant whose measurement method was proprietary.

Table 16. Statistics for participants' ferrule OD measurement offsets from NIST contact micrometer and ferrule concentricity measurement offsets from average values.

Participant	Outside diameter offsets from NIST contact micrometer		Concentricity offsets from average values	
	Average offset, μm	Standard deviation of offsets, μm	Average offset, μm	Standard deviation of offsets, μm
1	−0.55	0.24	+0.11	0.20
2	−0.27	0.25	+0.12	0.23
3	+0.14	0.27	+0.09	0.23
4	+0.31	0.16	−0.27	0.23
5	−0.26	0.12	+0.13	0.26
6	−0.19	0.11	−0.07	0.22
7	+0.34	0.21	−0.10	0.19
	Average offset magnitude,[a] μm	**Average offset spread,[b] μm**	**Average offset magnitude,[a] μm**	**Average offset spread,[b] μm**
	0.29	**0.19**	**0.13**	**0.22**

[a]Average of absolute values of participants' average offsets.

[b]Average of participants' offset standard deviations.
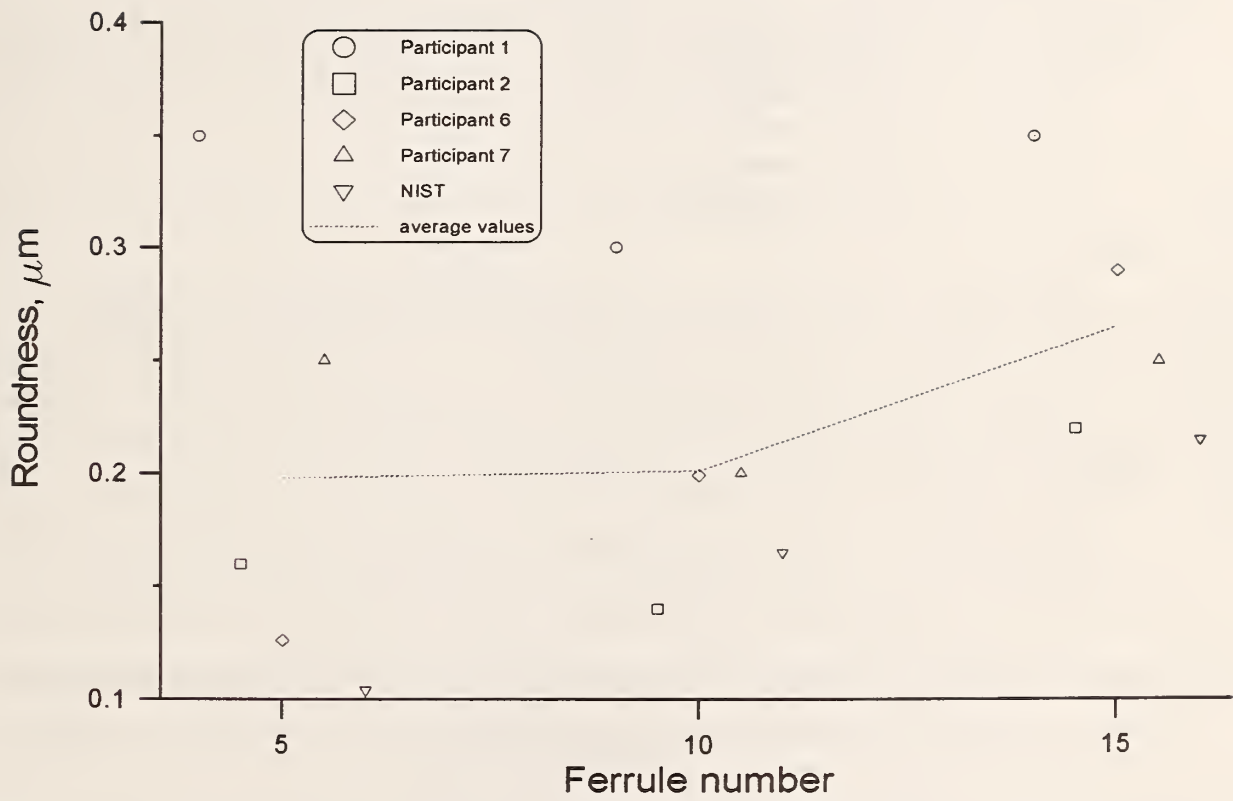
Figure 22. Ferrule roundness measurements on three ferrule specimens. Dotted line connects average values.
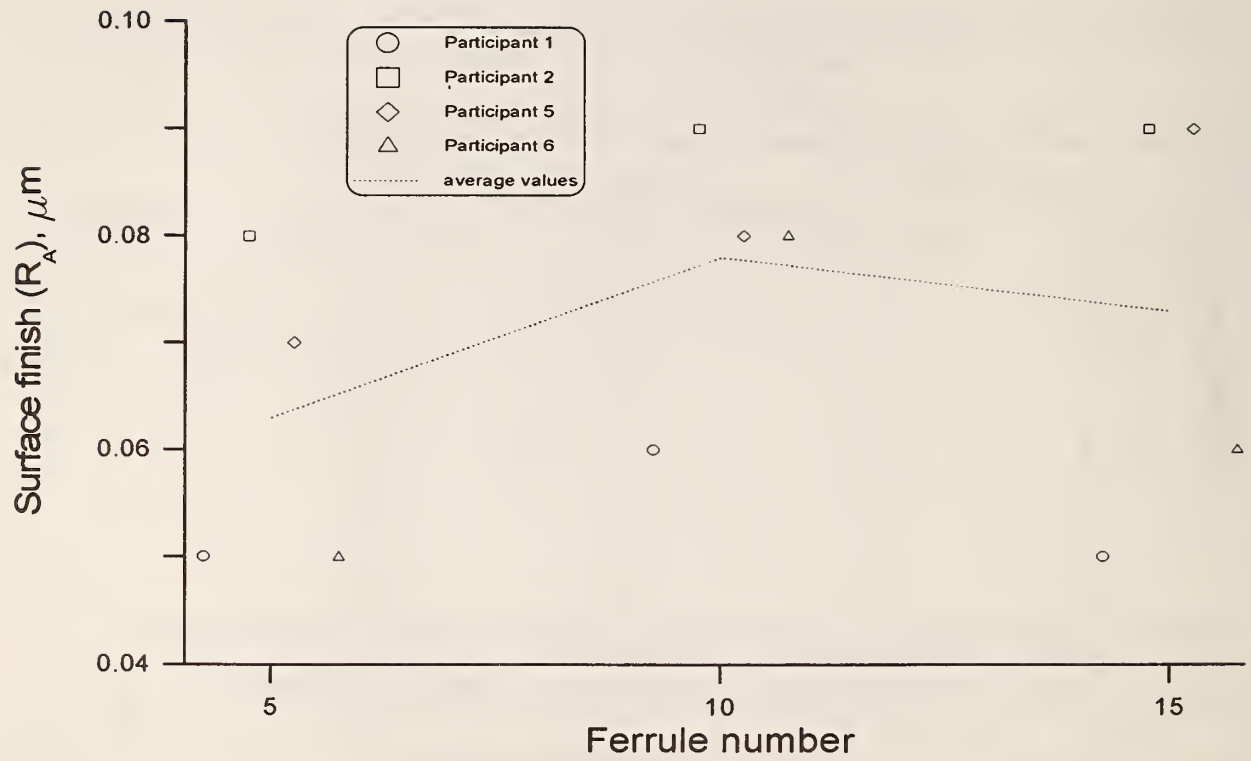
Figure 23. Ferrule surface finish measurements on three ferrule specimens. Dotted line connects average values.

4.4 Ferrule Endface Geometry—Future Work

The only remaining geometrical parameters of ferrules not addressed in previous sections are parameters related to ferrule/fiber endfaces in finished physical-contact connectors. These parameters are: fiber undercut/protrusion, which is the measurement of the longitudinal (axial) offset between the fiber endface and the ferrule endface; apex offset, which is a concentricity measurement of the transverse offset between the optical axis of the fiber and the peak (apex) of the spherically polished ferrule endface; and radius of curvature of the spherical ferrule endface. A TIA/NIST interlaboratory comparison of ferrule endface geometry measurements is currently (as of this writing) being planned and is expected to start by late 1995 or early 1996.

---

5. References

[1]   EIA-492B000, "Sectional Specification for Class IV Single-Mode Optical Waveguide Fibers," Telecommunications Industry Association—Electronic Industries Association, 2500 Wilson Blvd., Suite 300, Arlington, VA 22201; (703) 907-7700.

[2]   CCITT Study Group XV, "Results of a Round-Robin Study into Measurement of the Geometrical Properties of Single-Mode Fibres," September 1989.

[3]   Baines, John G. N.; Hallam, Andrew G.; Raine, Ken W.; Turner, Nick P., "Fiber Diameter Measurements and Their Calibration," *J. Lightwave Technol.*, vol. 8, no. 9, pp. 1259-1267, September 1990.

[4]   Drapela, Timothy J.; Franzen, Douglas L.; Young, Matt, "Single-Mode Fiber Geometry and Chromatic Dispersion: Results of Interlaboratory Comparisons," *Technical Digest: Symposium on Optical Fiber Measurements, 1992*, Natl. Inst. Stand. Technol. Spec. Publ. 839, ed. by G. W. Day and D. L. Franzen, pp. 187-190, September 1992.

[5]   National Institute of Standards and Technology, Standard Reference Material Program, Bldg. 2, Rm. 204, Gaithersburg, MD 20899; (301) 975-6776. Refer to SRM 2520, Optical Fiber Diameter Standard.

[6]   Young, Matt; Hale, Paul D.; Mechels, Steven E., "Optical Fiber Geometry: Accurate Measurement of Cladding Diameter," *J. Res. Natl. Inst. Stand. Technol.*, vol. 98, no. 2, pp. 203-216, March–April 1993.

[7]   TIA/EIA-455-176 (Fiberoptics Test Procedure FOTP-176), "Method for Measuring Optical Fiber Cross-Sectional Geometry by Automated Grey-Scale Analysis," Telecommunications Industry Association—Electronic Industries Association, 2500 Wilson Blvd., Suite 300, Arlington, VA 22201; (703) 907-7700.

[8]   Downs, M.J.; Turner, N.P., "Application of Microscopy to Dimensional Measurement in Microelectronics," *Proc. Soc. Photo-Opt. Instrum. Engrs.*, vol. 368, Microscopy—Techniques and Capabilities, pp. 82-87, 1982.

[9]   Baines, J.; Raine, K., "Review of Recent Developments in Fibre Geometry Measurements," *Technical Digest: Symposium on Optical Fiber Measurements, 1992*, Natl. Inst. Stand. Technol. Spec. Publ. 839, ed. by G. W. Day and D. L. Franzen, pp. 45-50, September 1992.

[10]   EIA/TIA-455-173 (Fiberoptics Test Procedure FOTP-173), "Coating Geometry Measurement for Optical Fiber, Side-View Method," Telecommunications Industry Association—Electronic Industries Association, 2500 Wilson Blvd., Suite 300, Arlington, VA 22201; (703) 907-7700.

[11]   TIA/EIA-455-163 (Fiberoptics Test Procedure FOTP-163), draft title: "Coating Geometry Measurement for Optical Fiber, Ray-Traced Side-View Method," Telecommunications Industry Association—Electronic Industries Association, 2500 Wilson Blvd., Suite 300, Arlington, VA 22201; (703) 907-7700.

[12]   TIA/EIA-455-119 (Fiberoptics Test Procedure FOTP-119), draft title: "Coating Geometry Measurement for Optical Fiber by Grey-Scale Analysis," Telecommunications Industry Association—Electronic Industries Association, 2500 Wilson Blvd., Suite 300, Arlington, VA 22201; (703) 907-7700.

[13]   TIA/EIA-455-93 (Fiberoptics Test Procedure FOTP-93), "Test Method for Optical Fiber Cladding Diameter and Noncircularity by Noncontacting Michelson Interferometry," Telecommunications Industry Association—Electronic Industries Association, 2500 Wilson Blvd., Suite 300, Arlington, VA 22201; (703) 907-7700.

[14]   TIA/EIA-455-*xxx* (unnumbered draft Fiberoptics Test Procedure FOTP-*xxx*), working title: "Connector Ferrule Hole Inside Diameter," Telecommunications Industry Association—Electronic Industries Association, 2500 Wilson Blvd., Suite 300, Arlington, VA 22201; (703) 907-7700, to be published.

[15]   National Institute of Standards and Technology, Standard Reference Material Program, Bldg. 2, Rm. 204, Gaithersburg, MD 20899; (301) 975-6776. Refer to SRM 2522, Pin Gage Standard for Optical Fiber Ferrules.

[16]   National Institute of Standards and Technology, Standard Reference Material Program, Bldg. 2, Rm. 204, Gaithersburg, MD 20899; (301) 975-6776. Refer to SRM 2523, Diameter Standard for Optical Fiber Ferrules.

[17]   TIA/EIA-604 (Fiber Optic Connector Intermateability Standards—FOCIS documents), Telecommunications Industry Association—Electronic Industries Association, 2500 Wilson Blvd., Suite 300, Arlington, VA 22201; (703) 907-7700.

[18]   TIA/EIA-455-*xxx* (unnumbered draft Fiberoptics Test Procedure FOTP-*xxx*), working title: "Connector Ferrule Inside and Outside Diameter Circular Runout," Telecommunications Industry Association—Electronic Industries Association, 2500 Wilson Blvd., Suite 300, Arlington, VA 22201; (703) 907-7700, to be published.

NIST Technical Publications

Periodical

Journal of Research of the National Institute of Standards and Technology—Reports NIST research and development in those disciplines of the physical and engineering sciences in which the Institute is active. These include physics, chemistry, engineering, mathematics, and computer sciences. Papers cover a broad range of subjects, with major emphasis on measurement methodology and the basic technology underlying standardization. Also included from time to time are survey articles on topics closely related to the Institute's technical and scientific programs. Issued six times a year.

Nonperiodicals

Monographs—Major contributions to the technical literature on various subjects related to the Institute's scientific and technical activities.

Handbooks—Recommended codes of engineering and industrial practice (including safety codes) developed in cooperation with interested industries, professional organizations, and regulatory bodies.

Special Publications—Include proceedings of conferences sponsored by NIST, NIST annual reports, and other special publications appropriate to this grouping such as wall charts, pocket cards, and bibliographies.

Applied Mathematics Series—Mathematical tables, manuals, and studies of special interest to physicists, engineers, chemists, biologists, mathematicians, computer programmers, and others engaged in scientific and technical work.

National Standard Reference Data Series—Provides quantitative data on the physical and chemical properties of materials, compiled from the world's literature and critically evaluated. Developed under a worldwide program coordinated by NIST under the authority of the National Standard Data Act (Public Law 90-396). NOTE: The Journal of Physical and Chemical Reference Data (JPCRD) is published bi-monthly for NIST by the American Chemical Society (ACS) and the American Institute of Physics (AIP). Subscriptions, reprints, and supplements are available from ACS, 1155 Sixteenth St., NW, Washington, DC 20056.

Building Science Series—Disseminates technical information developed at the Institute on building materials, components, systems, and whole structures. The series presents research results, test methods, and performance criteria related to the structural and environmental functions and the durability and safety characteristics of building elements and systems.

Technical Notes—Studies or reports which are complete in themselves but restrictive in their treatment of a subject. Analogous to monographs but not so comprehensive in scope or definitive in treatment of the subject area. Often serve as a vehicle for final reports of work performed at NIST under the sponsorship of other government agencies.

Voluntary Product Standards—Developed under procedures published by the Department of Commerce in Part 10, Title 15, of the Code of Federal Regulations. The standards establish nationally recognized requirements for products, and provide all concerned interests with a basis for common understanding of the characteristics of the products. NIST administers this program in support of the efforts of private-sector standardizing organizations.

Consumer Information Series—Practical information, based on NIST research and experience, covering areas of interest to the consumer. Easily understandable language and illustrations provide useful background knowledge for shopping in today's technological marketplace.
*Order the **above** NIST publications from: Superintendent of Documents, Government Printing Office, Washington, DC 20402.*
*Order the **following** NIST publications—FIPS and NISTIRs—from the National Technical Information Service, Springfield, VA 22161.*

Federal Information Processing Standards Publications (FIPS PUB)—Publications in this series collectively constitute the Federal Information Processing Standards Register. The Register serves as the official source of information in the Federal Government regarding standards issued by NIST pursuant to the Federal Property and Administrative Services Act of 1949 as amended, Public Law 89-306 (79 Stat. 1127), and as implemented by Executive Order 11717 (38 FR 12315, dated May 11, 1973) and Part 6 of Title 15 CFR (Code of Federal Regulations).

NIST Interagency Reports (NISTIR)—A special series of interim or final reports on work performed by NIST for outside sponsors (both government and non-government). In general, initial distribution is handled by the sponsor; public distribution is by the National Technical Information Service, Springfield, VA 22161, in paper copy or microfiche form.